Whole genome regulatory effect of *MoISW2* and consequences for the evolution of the rice plant pathogenic fungus *Magnaporthe oryzae*

Mengtian Pei[1*], Yakubu Saddeeq Abubakar[2,3], Hina Ali[1], Lianyu Lin[1], Xianying Dou[1], Guodong Lu[1], Zonghua Wang[1,4], Stefan Olsson[1,5*#], Ya Li[1#]

[1]State Key Laboratory of Ecological Pest Control for Fujian and Taiwan Crops, College of Plant Protection, Fujian Agriculture and Forestry University, Fuzhou 350002, China

[2]Key Laboratory for Plant-microbe Interaction, College of Life Sciences, Fujian Agriculture and Forestry University, Fuzhou 350002, China

[3]Department of Biochemistry, Faculty of Life Sciences, Ahmadu Bello University, Zaria 810103, Nigeria

[4]Institute of Oceanography, Minjiang University, Fuzhou, China

[5]Synthetic Biology Center, College of Future Technologies, Fujian Agriculture and Forestry University, Fuzhou 350002, China

*First authors Mengtian Pei and Stefan Olsson

#Corresponding authors:

Ya Li and Stefan Olsson

liya-81@163.com & Stefan@olssonstefan.com

Author contributions:

Mengtian Pei: ChIPseq and initial analyses; RNAseq and initial analyses; manuscript preparation and writing.

Yakubu Saddeq Abubakar: Constructive manuscript critique; manuscript corrections

Hina Ali: ChPseq; RNAseq

Lianyu Lin: Retrotransposon analysis of ChPseq data.

Xianying Dou: Constructive manuscript critique; manuscript corrections

Guodong Lu: Supervision; manuscript corrections

Zonghua Wang: Supervision; manuscript corrections

Ya Li: Obtaining funds; supervision; initial planning of experiments; construction of ISW2 mutant and phenotype analysis; manuscript preparation and writing

Stefan Olsson: ChIPseq and RNAseq extended analyses and synthesis; MEME, FungiFun, antiSMASH analyses; manuscript planning; manuscript preparation and writing.

Keywords: heterochromatin, epigenetics, nucleosomes, avirulence genes, retrotransposons, evolution

Abstract

Isw2 proteins are conserved in eukaryotes and are known to bind to DNA and dynamically influence local chromosome condensation close to their DNA binding site in an ATP-dependent manner making genes close to the binding sites more accessible for transcription and repression. A putative *MoISW2* gene was deleted with large effects on plant pathogenicity as a result. The gene was complemented and a ChIP-sec was performed to identify binding sites. RNAsec showed effects on the overall regulation of genes along the chromosomes for mutant and background strains and this was compared with RNAseq from 55 downloaded RNA-seq datasets from the same strain and found similar. MoIsw2 binding and activities create genomic regions affected by MoIsw2 with high gene expression variability close to the MoIsw2 binding sites while surrounding regions have lower gene expression variability. The genes affected by the MoIsw2 activity are niche-determinant genes (secreted proteins, secondary metabolites and stress-coping genes) and avirulence genes. We further show that MoIsw2 binding sites with the DNA binding motifs coincide with known transposable elements (TE) making it likely that TE-transposition at the binding sites can affect the transcription profile of *M. oryze* in a strain-specific manner. We conclude that MoIsw2 is a likely candidate for a master regulator, regulating the dynamic balance between biomass growth genes (like housekeeping genes) and nich-determinant genes important for ecological fitness. Stress-induced TE

63 transposition is together with MoIsw2 activity a likely mechanism creating more
64 mutations and faster evolution of the niche-determinant genes than for
65 housekeeping genes.
66
67

Introduction

The eukaryotic genome is organized into condensed nucleosomes, limiting access to DNA for transcription factors and more loosely packed regions that are easier to access for interactions with DNA for transcription factors and repressors. The cellular inheritance of this pattern is the basis of animal cell line specialization during embryogenesis (Serrano et al. 2013). Thus, DNA accessibility in fungi also plays an essential role in determining which genes can be efficiently transcribed (Huang et al. 2021).

Imitation Switch 2 (ISW2) belongs to the Imitation SWItch) subfamily (Uniprot) of the SNF2 (Sucrose__Non-Fermentable)/RAD54 helicase family. ISW2 proteins contain a Myb/Sant domain close to their C-termini that binds DNA. A role as a transcription factor is the main role often implicated for the Myb-domain containing family proteins in eukaryotes and especially in plants (Wieser and Adams 1995; Mateos et al. 2006; Du et al. 2009; Dubos et al. 2010; Lin et al. 2011; Lin et al. 2012; Prouse and Campbell 2012; Ambawat et al. 2013; Pattabiraman and Gonda 2013; Kim et al. 2014; Baldoni et al. 2015; Dong et al. 2015; Liu et al. 2015; Roy 2016; Matheis et al. 2017; Valsecchi et al. 2017; Verma et al. 2017; Allan and Espley 2018; Mitra 2018; Wang et al. 2018; J. Li et al. 2019; Ma and Constabel 2019; Cao et al. 2020; Li et al. 2024).

88 A true Isw2 should be involved in gene regulation by regulating the
89 access to DNA for transcription factors and repressors through binding to
90 DNA and controlling nucleosome positioning instead of being a classic
91 transcription factor (TF) (Kagalwala et al. 2004; Fazzio et al. 2005; Hada et al.
92 2019). Generally, Isw2 proteins have a histone binding domain that
93 interacts with histone 4 of a nucleosome and a catalytic ATPase domain
94 close to the N-terminus that reacts with ATP and changes the Isw2 protein
95 conformation (Whitehouse et al. 2007; Hota and Bartholomew 2011; Dang et al.
96 2014) so that the nucleosome moves towards the Isw2 DNA binding site
97 (Fazzio et al. 2005), and in that way, transcription is regulated by changing
98 TF and repressor proteins access to DNA. Isw2 is thus involved in targeted
99 nucleosome positioning around these sites. As a consequence of this
100 targeted positioning, a localized nucleosome condensation is created that
101 negatively affects the regulation of the genes at the DNA binding site
102 (Whitehouse et al. 2007) but favours regulation a bit further away from it
103 (Fazzio et al. 2005; Donovan et al. 2021).

104 There has been much research into Isw2-like protein binding, but it
105 has become clear that *in vitro* mapping of Isw2 binding and nucleosome
106 positioning does not reflect what mechanistically occurs *in vivo* (Fazzio et
107 al. 2005; Donovan et al. 2021), or the very transient nature of the interaction
108 with His4 (Erdel et al. 2010; Erdel and Rippe 2011). The interaction is

109 transient in that the nucleosomes closest to the Isw2 binding sites get
110 dynamically positioned by very frequent (seconds) interaction with the
111 Isw2 protein in an ATP-dependent manner. The activity keeps the closest
112 nucleosome(s) almost immobile, while nucleosomes further away get more
113 freedom to move and genes there are easier to access and regulate. (Donovan
114 et al. 2021). Experiments have shown that both the largest subunits of the
115 Isw2 complex, Isw2, and Itc1, are needed for robust, target-specific binding
116 to DNA while Isw2 alone is sufficient for basal-level binding (Fazzio et al.
117 2005).

118 Furthermore, Isw2 is known to bind DNA preferentially at intergenic
119 regions (Whitehouse et al. 2007) where transposable elements (TEs) are
120 commonly located (TE target sites). These sites are staggered cut palindromic
121 target sites (Linheiro and Bergman 2008). In addition, TEs are involved in stress
122 adaptation and host specialization in *Verticillium dahliae* (Faino et al. 2016) as
123 well as in the rice blast fungus *Magnaporthe oryzae* studied here (Chadha and
124 Sharma 2014; Yoshida et al. 2016) and should especially be needed when the host
125 plant detects the fungus as a pathogen at the transition between the endophytic to
126 necrotrophic infection phase of the fungus and thereafter (Cao et al. 2022).

127 *ISW2* is highly expressed and often considered a "housekeeping" gene
128 stably expressed under normal conditions (Machné and Murray 2012). The stable
129 expression of housekeeping genes has recently been challenged, and many genes

130 traditionally considered stably expressed are unreliable when expressed outside
131 relatively narrow conditions. Thus better methods for selecting housekeeping
132 genes that better fit a specific set of conditions or tissues have been employed
133 (Stanton et al. 2017). On the other hand, the change in ratios of target genes to
134 housekeeping genes reflects the actual change in gene expression ratios of 2 genes
135 of interest. In a previous paper from our lab (Zhang, Zhang, Liu, et al. 2019), we
136 used correlations of expression profiles between genes of interest to probe
137 possible gene functions. That can be done in transcriptomic data from many labs
138 and is especially useful if the calculations are done for all data and not just average
139 value data. Then, also the variation between replicates can be used to calculate the
140 correlation between any two genes' expressions since these ratios reveal the
141 dependencies of one gene's expression on the other gene, or both genes'
142 expressions on a third. Using ratios of gene expressions can thus reveal putative
143 gene functions and help identify genes with specific putative functions that should
144 correlate with the expression of well-known orthologous genes (Zhang, Zhang, Liu,
145 et al. 2019).

146 In this study we studied the putative *MoISW2* in *M. oryzae* as an *ISW2*
147 gene that affects gene regulation close to the MoIsw2 protein binding sites in the
148 fungal genome. Deletion of the gene negatively affected pathogenicity and stress
149 tolerance. We further show that MoIsw2 binding is at TEs within the genome
150 and that genes close to the binding sites are more differentially regulated (up or
151 down). The affected genes are mainly niche-determinant genes; this, combined

152 with TE transpositions, is a likely mechanism for biased evolution (Monroe et
153 al. 2022) in *M. oryzae* with a faster mutation rate for affected genes.

154

155 **Results**

156

157 **Bioinformatics similarity and domain structure**

158 The protein encoded by the MGG_01012 gene is annotated as a putative
159 MoIsw2 in the NCBI database. From its N to C termini, Isw2 proteins
160 consist of DExx, Helicase C, HAND, SANT and SLIDE domains (Hopfner
161 et al. 2012) (Supplementary method 1 for further comparisons). Thus, the
162 MoIsw2 protein is most probably an Isw2 protein of the IswI and Isw2 type
163 (**Fig 1A)**

164

165 **Deletion phenotypes of *ΔMoisw2* mutant and subcellular localization of**
166 **the MoIsw2-GFP protein**

167 The *MoISW2* gene was deleted in the *M. oryzae* Ku80 background strain
168 and the deletion was confirmed by Southern blot (**Fig S1**). The effect of
169 this mutation on the vegetative growth of the fungus was tested on three
170 types of media namely complete medium (CM), minimal medium (MM)
171 and rice bran medium (RBM), after incubation at 28 ℃ for ten days. The
172 assays showed significantly decreased colony size of the mutant on all three

173 media when compared to the background strain Ku80 and the
174 complemented strain (*ΔMoisw2*/*MoISW2*) (**Fig. 1B**).

175 A standard panel of stress treatments added to the CM medium was
176 used to test whether the deletion of the *MoISW2* gene affected the fungal
177 growth rates on different stressing media (Li et al. 2014). The CM medium
178 without the addition of any stress-inducing agent was used as the control
179 medium. The *ΔMoisw2* mutants are strongly inhibited by both SDS (affects
180 membrane integrity) and NaCl (induces osmotic and ionic stress) compared
181 to the controls (**Fig. 1C)**, suggesting that membrane pumps depending on
182 the membrane potential might not be necessarily upregulated and working
183 well in the mutant (Gostinčar et al. 2011).

184 Furthermore, we tested the ability of the mutant to produce conidia,
185 which are essential for the spread of rice blast disease from plant to plant
186 in the field. We tested this by checking the abundance of conidiophores
187 (which bear conidia) in the various strains. While the WT and
188 complemented strains produced many conidiophores, each bearing many
189 conidia, the *ΔMoisw2* mutant only produced scanty conidiophores with
190 very few conidia (**Fig. 1E**).

191 Next, the *ΔMoisw2* mutant was tested for pathogenicity on rice and
192 barley leaves and compared with the Ku80 background strain and
193 *ΔMoisw2*/*MoISW2* complemented strain**.** Since the *ΔMoisw2* mutant
194 produces too few conidia to be used for inoculation, agar plugs were used

195 to infect healthy rice and barley leaves in the infection assay. The assay
196 showed no infection for the *ΔMoisw2* mutant strains (**Fig. 1D**). We
197 reasoned that this could be due to an inability of the mutant to penetrate the
198 plant cuticles. Therefore, we inoculated the fungal strains on aseptically
199 wounded leaves and found that the *ΔMoisw2* mutant could not develop any
200 obvious disease symptoms on the leaves, indicating that *MoISW2* is needed
201 for any successful infection of rice or barley leaves **(Fig. 1D**). From
202 hyphae, *M. oryzae* can form appressoria needed for leaf infection. We
203 found however that dark appressoria formation was not affected by the
204 *MoISW2* mutation, confirming that the cause of no infection in the infection
205 assay was probably not a complete lack of appressoria formation (**Fig. 1E**).
206 Finally, the Moisw2/*MoISW2-GFP* complementation was used to
207 visualize the subcellular localization of MoIsw2. This was performed in a
208 strain expressing Histon1-mCherry (RFP) (as a nuclear marker)(Zhang,
209 Zhang, Chen, et al. 2019) because we expected that MoIsw2-GFP should
210 accumulate in the nucleus as its orthologues do in other eucaryotes. The
211 MoIsw2 protein was observed to consistently colocalize with the nuclear
212 marker in hyphae, conidia and appressoria (**Fig. 1F**).
213 Taken together, these results suggest that MoIsw2 localize to nuclei
214 and directly or indirectly regulates genes encoding proteins that in several
215 ways strengthen the cell wall and cell membrane barrier important for

216 growth inside a plant and might explain why the deletion of the gene
217 decreased the pathogenicity of the fungus.
218
219 **Correlation analyses of *ISW2* expression with expressions of nucleosome**
220 **histones and ITC1**
221 Histone 1 (*HIS1* gene) is involved in epigenetic activities by changing access to
222 DNA, and its expression is linked to silencing activity (Willcockson et al. 2021).
223 The active Isw2 protein complex containing Itc1 binds DNA and Histone 4
224 (Donovan et al. 2021) also affects access to DNA. We used downloaded published
225 expression data from the course of rice leaf infection from many experiments for
226 the strain we use to investigate correlations between the putative *MoISW2* and the
227 MoIsw2 complex gene candidates in the same way as we have done before for
228 other genes using the same data (Zhang, Zhang, Liu, et al. 2019). We now
229 investigate if the putative *MoISW2* is transcriptionally coregulated with genes that
230 encode proteins MoIsw2 need to interact with to perform MoIsw2 local site-
231 specific epigenetic activities. The *MoHIS1* expression increases steeply with
232 *MoISW2* gene expression (**Fig. 2**). In *M. oryzae,* there are two genes
233 (MGG_06293 and MGG_01160) *MoHIS4a* and *MoHIS4b* respectively that are
234 predicted (NCBI) to encode an identical His4 protein. Thus the sum of these gene
235 regulations should best reflect the regulation of the MoHis4 protein. Isw2 further
236 works together with ITC1 in a complex that interacts with His4 (Kagalwala et al.
237 2004). Thus, the expression of these 4 putative genes (*MoISW2*, *MoITC1* and

238 *MoHIS4a+MoHIS4b*) producing 3 proteins (MoIsw2, MoItc1 and MoHis4)
239 should be correlated in *M. oryzae,* and they are nicely correlated in the data from
240 plant infection (**Fig. 2** and **Fig S2**). The closest correlation of *MoISW2* expression
241 is even with *MoHIS4a+MoHIS4b.* Thus, it points to that the putative MoIsw2 is a
242 real Isw2 as these proteins encoded by these genes are known to interact with His1,
243 Itc1 and His4 in a complex (Fazzio et al. 2005). Furthermore, the expression of
244 *MoHIS2B* is related to the overall growth rate (and thus *de novo* DNA synthesis
245 rate) (Zhang, Zhang, Liu, et al. 2019) and is correlated with *MoISW2* but not with
246 a steep slope. This points to that a smaller amount of MoHis2B is needed than
247 His4 for handling the de novo DNA synthesis per cell than what is needed when
248 Isw2 activity is high. That in turn could mean a lowering of the DNA-synthesis
249 rate with higher *MoISW2* expression. Also, the expression of *MoHIS3* but not
250 *MoHIS2A* is significantly correlated with the putative *MoISW2*. **(Fig. S3).**
251 Although the MoIsw2 protein interacts directly with His4 according to the
252 literature such interactions could not be detected using a yeast two-hybrid assay
253 (data not shown) and the lack of positive results in this assay is likely due to the
254 very transient nature of the interaction (Erdel et al. 2010; Erdel and Rippe 2011).
255 Thus, the putative *MoISW2* gene likely encodes a putative MoIsw2 protein
256 involved in targeted local chromatin compaction working with MoHis1, MoItc1
257 and MoHis4 (Fazzio et al. 2005; Donovan et al. 2021; Willcockson et al. 2021).
258 2021). From now on, we skip "putative" as an attribute and investigate if MoIsw2

259 has the expected functions as an Isw2 and what other effects it has on the biology
260 of the fungus. Furthermore, the local chromatin compaction and the regulatory
261 effect caused by MoIsw2 should be dynamic and stronger the more the gene and
262 the protein it encodes are expressed, and the more ATP there is available for the
263 dynamic interaction.
264
265 **ChIP-seq analysis of MoIsw2 finds DNA binding motifs**
266
267 We made a MoIsw2-GFP fusion protein to perform a ChIP-seq analysis to find
268 conserved DNA binding palindromic motifs for the binding of MoIsw2 to *M.*
269 *oryzae* DNA sequences.
270 As mentioned in the introduction, Isw2 proteins are known to preferentially
271 bind DNA at intergenic regions where transposable elements (TEs) are commonly
272 located (Whitehouse et al. 2007) with staggered palindromic motif target sites
273 (Linheiro and Bergman 2008). TEs are also mainly located intergenic in *M. oryzae*
274 in previous unmapped DNA (Chadha and Sharma 2014; Bao et al. 2017) and
275 appear to affect secreted protein expression important for pathogenesis differently
276 in different *M. oryzae* strains (Bao et al. 2017).
277 Our new data showed hits mainly for intergenic sequences (**Supplemental**
278 **Data 1**) where the palindromic retrotransposon sequences are preferentially
279 located (Linheiro and Bergman 2008). For these reasons, we looked for
280 palindromic motifs in the ChIP-seq sequences interacting with MoIsw2-GFP. For

281 this analysis we used the MEME website and as input all sequences (peaks) with
282 the ChIP-seq sequences. In addition, we also searched the ChIP-seq sequences for
283 previously identified RT sequences (Bao et al. 2017).

284 Three palindromic motifs were found to be common (**Supplemental Data**
285 **2**) with 47, 196 (**Fig. 2F)**, and 32 occurrences for motifs 1, 2 and 3 respectively,
286 located at 267 DNA locations. The large majority of these locations are intergenic
287 and only a few ChIP-seq sequences had more than one motif hit. We investigated
288 in detail the motif with 196 hits and the majority of these hits were indeed
289 intergenic (113 intergenic locations), while the rest (63) were in the promoter
290 region of a gene. Using a TOMTOM search at the MEME website, we found that
291 the most common palindromic motif 2 is similar to a known human Myb-binding
292 protein containing a DNA binding motif (**Fig. S4, Supplemental Data 3**).

293

294 **MoIsw2 DNA binding and its influence on close-by avirulence gene**
295 **expression.**

296 Transposable elements interacting with MoIsw2 may play a direct role in a
297 pathogen-plant arms race if they affect the expression of the nearby avirulence
298 genes (Chadha and Sharma 2014; Bao et al. 2017) through targeted nucleosome
299 condensation (Bourras et al. 2016; Fijarczyk et al. 2022; Feurtey et al. 2023).
300 Avirulence genes are often effectors the pathogen needs to efficiently cause
301 disease and parasitize the host, but different cultivars of the host acquire resistance
302 against these proteins naturally or through human exploitation in plant breeding

303 programs to develop disease-resistant plant varieties (Jones and Dangl 2006). For
304 these reasons, avirulence genes should preferably have become placed adjacent to
305 the MoIsw2 binding site through evolution, and their expression should be
306 affected differently depending on their closeness to the MoIsw2 binding site.

307 We first made a list of all known avirulence genes noted for *M. oryzae* at
308 NCBI (**Table 1, Supplemental data 9**) to test the above. There are 16 avirulence
309 genes of different types and in addition, the avirulence gene cluster of 12 more
310 genes for a cytochalasan-type compound biosynthesis (Collemare et al. 2008;
311 Song et al. 2015). We then made an RNAseq of the background strain *Ku80* and
312 compared it with the *MoISW2* mutant which also could be compared with the
313 downloaded data. The cytochalasan cluster is specifically activated at early hours
314 post-infection (HPI) during penetration and produces a secondary metabolite
315 recognized by the *R* gene *Pi33* in resistant rice cultivars (Collemare et al. 2008).
316 Two other avirulence genes, Avr-PWL1 and Avr-PWL2 (Dioh et al. 2000),
317 together with the previous, make 18 classic avirulence-type genes, excluding the
318 cytochalasan gene cluster genes (**Table 1**). Most of the genes in the cytochalasan
319 cluster are very closely positioned to MoIsw2 palindromic DNA binding motif
320 sites, and several are differently expressed in strains Guy11 and 98-06 (**Table 1**),
321 which might lead to the production of different final metabolites from the
322 cytochalasan gene cluster even if the different metabolites function as virulence
323 factors.

324 Six other avirulence genes are not expressed in either strain (**Table 1**). Of
325 these 6 genes, half of the genes are close to the MoIsw2 binding site, and 3 are
326 further away in Guy11. Two avirulence genes (MGG_17614 and MGG_15611)
327 are in supercontigs with unknown gene order in our data, so it is unsure how far
328 they are from a MoIsw2 binding site.
329
330 **TE position and MoIsw2 DNA binding**
331
332 We searched the short MoISW2 ChIPseq sequences data for described TEs
333 sequences (Bao et al. 2017) and found described TEs in 92.2 per cent of sequences
334 while the genome outside these ChIPseq sequences is almost devoid of TEs
335 (**Supplemental data 5**). We mapped the MoIsw2 binding sites to the genome as
336 well as the position of all found transposable elements (TEs) (**Fig. 3**). The
337 positioning of the MoIsw2 binding sites and the palindromic motifs we
338 found are close to retrotransposons and the differential regulation. The
339 found expression variation can indicate that MoIsw2-specific targeting is
340 instrumental for stabilizing avirulence gene expression. These data and
341 analyses with additional references are available in supplemental data files
342 (**Supplemental data 4 and 5**). In conclusion, MoIsw2 and RT activities could
343 together be instrumental in creating variation in gene expression profiles between
344 fungal strains.
345

346 **MoIsw2 regulates the genes closest to the MoIsw2 motif sites in the DNA**

347

348 We next compared the RNAseq for the *Δmoisw2* strain and the background *Ku80*
349 strain for overall gene regulations (**Fig. 4A-B**). There was a general upregulation
350 of the genes closest to the MoIsw2 binding sites in the *ΔMoisw2* mutant (**Fig. 4A**).
351 For these genes, the *ΔMoisw2*/*Ku80* expression ratio is lower when the MoIsw2
352 is predicted to bind directly in the promoter region than for the closest gene for a
353 predicted intergenic binding of MoIsw2. On the other hand, if absolute (positive
354 or negative) regulation was considered both types of genes, with MoIsw2 binding
355 in the promoter region or intergenic, had similar absolute regulation indicating
356 that many genes with MoIsw2 binding in their promoter region are repressed in
357 *ΔMoisw2*. This suggests that without MoIsw2 activity, repressors can also get
358 access to the DNA (**Fig. 4B**). These observations support MoIsw2 as an Isw2
359 protein that creates a local nucleosome condensation at specific nucleosomes
360 (Donovan et al. 2021) increasing genes' either transcriptions or repressions at
361 slightly further distances from the DNA binding sites.

362

363 **Overall functional classification of differentially expressed genes in the**
364 **RNA-seq data**

365

366 In *ΔMoisw2* grown on MM-medium, 339 genes were significantly
367 upregulated relative to the background *Ku80*. The two largest significantly

368 overrepresented gene categories were secondary metabolism and DNA-
369 binding, while most other categories are related to DNA synthesis, DNA-
370 linked activities and other growth-related processes (anabolism) (**Fig. 4C**).
371 These are the genes MoIsw2 likely negatively regulates in the background
372 *Ku80*. Most downregulated genes in the *ΔMoisw2* are genes involved in
373 mitochondrial electron transport, other mitochondrial processes,
374 transported compounds and other processes connected with uptake and
375 respiration and oxidative phosphorylation (catabolism) (**Fig. 4E**).
376 In other words, our results indicate that MoIsw2 is involved in
377 regulating the balance between anabolism and catabolism. Between DNA
378 synthesis, which is safest without ATP generation by mitochondrial
379 respiration since that generates Radical Oxygen Species (ROS), and
380 oxidative phosphorylation, which is more effective in generating ATP from
381 the metabolized substrates (Klevecz et al. 2004).
382
383 **The local gene regulations close to the MoIsw2 palindromic DNA binding**
384 **sites fit the Isw2-specific targeted DNA binding model.**
385
386 DNA is wrapped around and slides around nucleosomes of similar sizes, with a
387 constant overall Nucleosome Repeat Length (NRL) (van Holde 1989; Cutter and
388 Hayes 2015; Donovan et al. 2021; Willcockson et al. 2021) and NRLs sizes vary
389 slightly depending on the organism, cell type and cell status (van Holde 1989).

390 To further investigate local regulation around at or close to the binding sites with
391 the found palindromic motif, we investigated our RNAseq data and ordered the
392 MGG-codes for the genes in the order of the genes on the chromosomes
393 (Chromosome order downloaded from BROAD).

394 Dynamic changes due to chromosome packing affected by MoIsw2 should
395 result in the same regulatory landscape in ween in our experiment and the
396 downloaded data. Since MoIsw2 activity depends on respiratory catabolism
397 activity (nutrient availability in the niche) as mentioned above, the greatest
398 variation in expression between experiments should be for genes positioned close
399 to the MoIsw2 binding sites in the DNA. The change of the measured gene
400 expression responses in our RNAsec data and compared expression responses
401 (positive and negative) in Ku80 (background) strain with the *ΔMoisw2* mutant
402 strain (DelR). We could then test if the variation in expression responses (positive
403 and negative) (VarR) in the downloaded data from 55 RNAsec datasets from
404 several labs shows expression variations at similar positions in the data as were
405 affected by the deletion. We found that the two gene expression measurements
406 were Log-Log correlated (P=5.3E-196) and that the response slope of the
407 correlation was 0.56 with VarR on the x-axis (**Fig. S5, Supplemental Data 11**).

408 We further calculated the gene distance between each gene and the closest
409 MoIsw2 binding site (**Supplemental Data 10**) and plotted that together with plots
410 of the gene expression change from our experiment (DelR) and the variation in
411 the downloaded data (VarR). In the plot (**Fig. 5**), we also included the positions

412 of the avirulence genes (rings). From these comparisons, one can see that gene
413 regulatory responses along the genome are dependent on MoIsw2 and its binding
414 to DNA. Further, we can identify regions along the DNA with high variation in
415 gene regulation between experiments close (less than 16 genes from the closest
416 motif) to MoIsw2 binding motifs (**Fig. 5** Regions (A-U)) and regions with less
417 variation further away (17-to about 500 genes) from the MoIsw2 binding motifs
418 (**Fig. 5** Regions (1-15)). In **Figure 5** we have marked the positions of the Avir
419 genes as well.

420 For typical housekeeping genes like the genes encoding ribosomal proteins
421 (Zhang, Zhang, Liu, et al. 2019), their expression depends on the overall rate of
422 translation and should be quite constant between experiments. These genes are
423 mainly found further away from the MoIsw2 binding sites and TEs confirming
424 that the ribosomal proteins are in regions with more stable expression (**Fig. 6A**).

425 On the other hand, genes that are important for interaction with the
426 environment as the secreted proteins with identified domains (SP) and smaller
427 other secreted proteins (OSP) (Bao et al. 2017) are positioned in the more variable
428 genomic regions closer to the MoIsw2 binding motifs (**Fig. 6B** and **6C,**
429 **Supplemental Data 6-7**)

430 Other genes that are important in interaction with the environment are
431 secondary metabolites. Instead of searching the literature, we used the AntiSmash
432 web server and submitted the whole DNA sequence from BROAD to get a more
433 extensive list of putative core secondary metabolite genes. We found 64 core

434 secondary metabolite genes and plotted their positions along the ordered gene
435 positions (**Fig. 7A, Supplemental Data 8**) and found that they are mainly
436 positioned close to MoIw2 binding motif sites.

437 Epigenetic silencing can if it is persistent from generation to generation
438 result in the silenced genes accumulating deleterious mutations since the genes
439 are never expressed and needed in the ecological niche the organism lives in. We
440 consider genes not expressed in any of the downloaded RNAsec datasets as
441 potential pseudogenes (PP). Since the misuse of the pseudogene term does not
442 make sense, we follow the nomenclature suggested (Cheetham, Faulkner, and
443 Dinger 2020) and only use the term pseudogene alone for sequences that look like
444 genes and are not expressed at all under natural conditions. Consequently, due to
445 limited knowledge of most microorganisms' natural lifecycles, it is difficult to
446 definitively classify a gene as a vestigial gene or a pseudogene. However, if a
447 gene is rarely expressed under natural evolutionary relevant circumstances and
448 accumulates mutations over time rendering it non-functional, it may eventually
449 become a pseudogene. Several genes close to the *MoISW2* binding sites were not
450 expressed at all in any of the 54 downloaded RNAseq datasets (**Fig. 6B** and
451 **Supplementary Data 4)** indicating that these genes could be or become vestigial
452 genes or pseudogenes without biological roles, thus we call them potential
453 pseudogenes following the definition for the pseudogene concept recently
454 suggested (Cheetham et al. 2020). Our observation that these genes are or have
455 become potential pseudogenes during evolution is exciting since some of these

456 genes close to the MoIsw2 binding sites are annotated as avirulence effector genes
457 (**see Table 1**).
458
459 **DNA binding genes**
460 Since 65 genes were classified as DNA-binding and were among the
461 enriched genes upregulated in *ΔMoisw2* (**Fig. 3C, Supplemental Data 13**)
462 these could be conventional TFs, suppressors or other DNA binding genes
463 needed when interacting with the biotic and abiotic environment potentially
464 of high importance during pathogenesis.
465 The 12 DNA-binding genes most suppressed by MoIsw2 activity are
466 mainly involved in DNA repair (**Table 2**) needed for DNA synthesis and growth.
467 Among the most regulated genes were two TFs and several helicases as well as
468 other genes needed for DNA repair during and after DNA synthesis. A fungal-
469 specific gene involved in (sexual) sporulation is also in this list of 12 DNA-
470 binding genes most suppressed by the MoIsw2 activity.
471
472 **Functional classification of genes potentially affected by the MoIw2 activity**
473
474 **A. Genes at the MoIsw2 binding sites in DNA sequences**
475 We have above shown that genes under *MoISW2* control that are more expressed
476 in the background *Ku80* strain compared to the *ΔMoisw2* strain are enriched for
477 gene classes associated with secondary metabolism as well as biomass growth

478 (anabolism) while the genes that are downregulated in the mutant are connected
479 to aerobic metabolism and stress (**Fig. 3C**).

480 Using the *MoISW2* ChIP-seq data, we investigated the FunCat
481 classification of all genes adjacent to or in ChIP sequence hits to find out what
482 types of genes are overrepresented and which are depleted. First, we removed
483 double ChIP peak sequence hits close to the same gene so as not to count the same
484 gene twice. We then investigated the list of genes that are closest to the found
485 MoIsw2 binding sites. These genes should be targeted by MoIsw2 and might be
486 under positive or negative control from MoIsw2. According to the previous
487 analysis, they should not belong to growth (anabolism) but be genes active when
488 oxygen is consumed, and the substrates oxidized (catabolism) (Klevecz et al. 2004;
489 Machné and Murray 2012). In addition, the binding sequences are located close
490 to avirulence genes and retrotransposons, so their regulation can shift depending
491 on retrotransposon transpositions. Note that since ChIP-seq only shows potential
492 binding to DNA *in vitro,* we cannot say if these genes are up or downregulated;
493 only that a regulation influenced by MoIsw2 is possible.

494 Genes with ChIP binding hits closest to the MoIsw2 palindromic DNA
495 binding motif site are mainly enriched for genes involved in secondary
496 metabolism and other gene classes important for biotic interactions (**Fig. 7A)**. In
497 contrast, categories of genes for biomass growth and housekeeping (anabolism)
498 are depleted (**Fig. 7B**).

499 Many other genes within ChIP-seq sequences could be affected. These
500 genes are many more than those closest to the MoIsw2 palindromic DNA motif2
501 sites. For these (**Fig. 7C**)., we find more gene classes including detoxification
502 and signalling (cyclic nucleotide-binding), disease, and defence, and these are
503 all important gene classes involved in biotic and abiotic interactions with the
504 environments. Depleted are gene classes characteristic for anabolism (biomass
505 growth) (**Fig. 7D**).
506 Finally, the genes in the ChIP-seq data but not with motif2 hits (not
507 containing the MoIsw2 palindromic DNA binding motif 2 sites) are again genes
508 enriched for secondary genes and again genes involved in abiotic and biotic
509 interactions (**Fig. 7E**). Genes needed for biomass growth are depleted (**Fig. 7F**).
510
511 **Functional classification of 500 genes showing the highest VarR and DelR**
512 **values.**
513
514 As we have seen above (**Fig. 7**) the genes close to MoIisw2 binding motif123 are
515 in general more variable expressed DNA regions between RNAsec plant infection
516 experiments (VarR). These regions number the most TEs and core secondary
517 metabolite genes. To get more information on functional classes regulated we
518 used FungiFun again and did a functional classification of the 500 most variable
519 genes (VarR) in the downloaded data and compared that with the genes most
520 affected by the *MoISW2* deletion (**Fig. 9, Supplemental Data 12**). Few of these

521 genes are probably directly regulated by MoIsw2 but the access to them for gene
522 regulation should be affected. Furthermore, similarities and differences between
523 VarR and DelR should point to regulations biased for genes important for plant
524 interactions or plate growth respectively.

525 Genes categories needed to cope with the abiotic and biotic environment
526 are enriched among the 500 with the highest VarR **and** DelR values indicating
527 that both the lab and inside plants' similar gene functions are in principle affected
528 by the MoIsw2 activities (**Fig 9A**). Depleted functional gene classes are growth-
529 related genes (anabolic) and some stress-related genes (**Fig 9B**).

530 Genes categories needed to cope with the abiotic and biotic environment
531 are again enriched among the VarR 500 most differentially regulated gene classes
532 (**Fig. 9C**). Depleted are again growth-related genes (anabolic) and stress-related
533 gene classes (**Fig. 9D**).

534 The fungal biomass had recently been shifted from stationary (agar plugs)
535 with the nuclei in various states of growth to a liquid medium for 48h triggering
536 vigorous growth. Thus, variations in the genes affected by the deletion (DelR) are
537 expected in genes for how fast the biomass reacts to the new situation of plenty
538 of nutrients also for genes not affected by MoIsw2 activities. That is probably
539 why unfolded protein response genes are among the enriched genes most affected
540 by the deletion in DelR (**Fig. 9E**), . But in general, the functional gene classes
541 among the most regulated VarR alone and most deletion-affected DelR alone are
542 similar.

543 The specifically differential regulation during plant infection (VarR-
544 specific genes) are genes that are expected to be genes classes responding in
545 fungal-innate immunity (Ipcho et al. 2016) (reacting to plants in this case) (**Fig.**
546 **10A-B**) and are further discussed in the discussion section. The DelR-specific
547 enriched and depleted gene classes (**Fig. 10 C-D**) indicate gene classes important
548 to regulate during fast aerobic growth of hyphal biomass and nutrient uptake from
549 the environment *in vitro*.

550 **Discussion**

551

552 **Deletion effects on phenotypes, and regulation (DelR) compared with**
553 **variability in regulation between RNAseq experiments (VarR).**

554 When *MoISW2* is deleted, the general growth of the fungus (**Fig. 1**) was
555 negatively affected, as was the sensitivity to SDS and NaCl. Conidiation
556 was completely abolished as was also pathogenicity, and the MoIsw2-GFP
557 fusion accumulates in the nucleus as expected for a nuclear localized
558 protein. The strong effect on infection and the fact that Isw2 proteins are
559 known to affect the regulation of many genes in genomes through local
560 chromosomes around several DNA binding sites (Fazzio et al. 2005)
561 indicates that *MoISW2* could be a "master regulator" for regulating the many
562 fungal defences against the plant defences. This is because these and virulence
563 factors (for example secondary metabolism) are especially upregulated in the
564 biotrophy/necrotrophy transition, and during the necrotrophic stage (Andrew et al.

565 2012; Kou et al. 2019) when membrane effects on the pathogens are especially
566 prominent and the fungus have to deal with plant ROS defences.

567 We found that potential effector genes like avirulence genes, secreted
568 proteins, and core secondary metabolite genes are located in the DNA regions that
569 appear to be under MoIsw2 control. The protein appears to have the role of a
570 master regulator of TF and repressor gene access to genes necessary for the fungus
571 reacting with the biotic and abiotic environment (**Fig. 5, 6, 7A**) since these gene
572 types are in regions of the DNA that are differentially regulated in the *ΔMoisw2*
573 compared to the background K80 (DelR). These regions are also the same regions
574 with the highest variability between experiments in a set of RNAseq data from 55
575 downloaded RNAseq datasets from experiments in planta (**Fig. 5**) (VarR). That
576 is what could be expected for nich determinant genes that are not involved in the
577 basic metabolism.

578 The overall regulation effect of all genes in the two datasets (VarR and
579 DelR) were correlated as they should be if the regulated regions in the two datasets
580 were the same and strain-specific and not experiment-specific and only dependent
581 on the MoIsw2 activity caused organisation of chromatin in the particular strain.
582 Growth inside a plant is stressful for a plant pathogen. The fungus must
583 compete with the plant for all nutrients during the biotrophic stage without
584 revealing its existence and then trigger plant immunity responses that it has
585 to handle in the necrotrophic stage (Andrew et al. 2012; Chowdhury et al. 2017;
586 Rajarammohan 2021). When shifting to the necrotrophic stage the

587 pathogenic fungus must thus both overcome plant defences and nutrient
588 limitations since when spreading inside the plant, nutrient limitations might
589 occur (Josefsen et al. 2012). In support of a strain-specific "master regulator"
590 function for MoIsw2 regulating responses to environmental conditions, we find
591 that many fungal defence and virulence-related functional gene classes are
592 regulated and positioned in the variably regulated chromosomal regions that
593 appear to be under MoIsw2 activity control (**Fig. 8 and 9**). There is in addition a
594 difference in the regulation of avirulence genes between *M. oryzae* strains and
595 these genes are situated close to the MoIsw2 binding sites in the DNA giving the
596 strain specificity of the MoIsw2 as master regulator further support (**Table 1**).
597
598 **Regulation of chromatin condensation by nucleosome positioning**
599
600 **MoIsw2 is a true Isw2**
601 Direct interactions with His4 could not be detected by a yeast two-hybrid
602 assay. The yeast Isw1 and Isw2 interactions with His4 are transient
603 (approximately 200 and 80 bindings per minute, respectively) and need a
604 continuous ATP supply (Tsukiyama et al. 1999). Similarly, the interaction in
605 human cells has been measured in vivo using advanced microscopy and
606 spectroscopy techniques and found to be transient (10-150ms)(Erdel et al.
607 2010; Erdel and Rippe 2011). Thus, our attempts to detect an interaction
608 between MoIsw2 and MoHis4 using the yeast two-hybrid method were in

609 vain. On the other hand, the expression of MoIsw2 and the expression of
610 orthologues to genes in *M. oryzae,* that an Isw2 protein are known to
611 physically interact and form a functional Isw2 protein complex (Donovan et
612 al. 2021), are correlated (**Fig. 2**). That indicates that MoIsw2 is a true Isw2
613 with a conserved Isw2 protein function and it has a conserved order of
614 domains in the protein (**Fig. 1A**)
615

616 **Regulation of MoIsw2 activity and regulation by *MoISW2* expression**

617 Isw1 translocates nucleosomes away from other nucleosomes, while Isw2
618 translocates towards the centre of DNA pieces and other nucleosomes *in*
619 *vitro,* with the nucleosomes bound to relatively short DNA pieces
620 (Kagalwala et al. 2004; Zofall et al. 2004). It does the same *in vivo* where it
621 was found that Isw2 is mainly involved in the targeted regulation of DNA
622 access close to the Isw2 DNA binding site (Fazzio et al. 2005), as we also
623 find (**Fig. 4, Table 1**).

624 The Isw2 activity is ATP dependent (Whitehouse et al. 2007; Hota and
625 Bartholomew 2011; Dang et al. 2014). Thus the regulation of genes adjacent
626 to the DNA-binding site is likely to be highly dependent on ATP
627 availability and competition for ATP in the cytoplasm-nucleus
628 compartment. ATP generation from fermentation is much faster but less
629 efficient than from oxidative phosphorylation when fast fermentation is
630 possible. In yeast, growth is characterized by DNA replication, mainly

631 without mitochondrial oxidative activity (fast aerobic glycolysis), most
632 probably to protect DNA from mutations (Klevecz et al. 2004). In *M. oryzae,*
633 MoIsw2 could thus be an ATP-regulated switch (Machné and Murray 2012)
634 between fast aerobic glycolysis accompanied by DNA-synthesis growth
635 with quality control, and slower but more efficient oxidative
636 phosphorylation growth with high ATP yield, active oxidative defences,
637 and interaction with the abiotic and biotic environment that makes up the
638 *M. oryzae* ecological niche. In support of this, we found that genes
639 upregulated in the *ΔMoisw2* mutant and thus repressed by MoIsw2 under
640 other more ATP-limited aerobic growth conditions are involved in fast
641 growth and DNA synthesis, DNA quality control, while downregulated
642 genes in the mutant were those involved in oxidative phosphorylation,
643 stress management, and secondary metabolite biosynthesis (**Fig. 3EF** and
644 **Table 2**). As also expected from the known function of Isw2, the genes
645 closest to the two central immobilized nucleosomes at the MoIsw2 DNA-
646 binding sites are downregulated in the background *Ku80* (Donovan et al.
647 2021), and when *MoISW2* is deleted, these genes are upregulated (**Fig. 3A**).
648

649 **Regulation by MoIsw2 is dependent on distance from the MoIsw2 DNA**
650 **binding sites.**

651 Gene regulation affected in the *ΔMoisw2* mutant strain compared to the
652 background Ku80 strain (DelR) as well as the variation between RNAseq

653 experiments (VarR) are dependent on the distance from the MoIsw2 DNA
654 binding motif sites (**Fig. 5**). That agrees with that regulation is a
655 consequence of the MoIsw2 positioning of the closest nucleosomes giving
656 more sliding space to surrounding nucleosomes (Donovan et al. 2021) and
657 consequently increased DNA access. Genes affected by the MoIsw2 activities
658 and being physically close to the palindromic binding sites in the DNA are
659 for example genes for secreted protein while core secondary metabolites
660 while typical housekeeping genes like genes encoding ribosomal proteins
661 are much further away (**Fig. 6**). In support of this we found that the 500
662 most regulated genes (High VarR and/or DelR) with most variable gene
663 expression were significantly enriched for functional gene classes needed
664 to react to the biotic and abiotic environment and depleted for typical
665 housekeeping genes (**Fig. 9**). Interestingly, and in line with this
666 interpretation, the 500 genes specifically upregulated in VarR (during plant
667 pathogenesis) and in DelR (growth in vitro) are genes that reflect the two
668 different biotic/abiotic environments for the fungus. The functional gene
669 classes specially enriched in VarR (especially the ones in red text) are those
670 that are expected for fungal innate immunity (Ipcho et al. 2016) and
671 protection against plant innate immunity like the removal of fungal cell
672 wall derived aminosaccharides (chitin oligomers) that triggers plant
673 immunity (Nürnberger et al. 2004) (**Fig. 10A**).
674

675 **Conserved and variable DNA**

676 Our observations suggest that the *M. oryzae* genome is organized into
677 regions with constant expression and variable expression depending on the
678 environment. The regions with variable expression are close to MoIsw2
679 DNA binding sites and contain genes important for the interaction with the
680 environment (during biotic and abiotic stresses) while regions with less
681 variable expression contain housekeeping genes. Such a division of the
682 fungal genome into regions of housekeeping genes and niche-determinant
683 faster-evolving genes is consistent with previous findings in the relatively
684 closely related *Fusarium graminearu*m (Zhao et al. 2014) but also in *V.*
685 *dahliae* (Faino et al. 2016).

686 Palindromic sequences are characteristic of retrotransposons that are
687 mainly positioned close to stress-related genes and avirulence genes in the
688 genomes of fungal plant pathogens. Fungal avirulence genes are plant-
689 pathogen effectors that trigger different plant immunity responses
690 depending on plant variety and the basis for plant cultivar-specific
691 resistance to specific pathogen strains (the gene-for-gene relationship)
692 (Bourras et al. 2016) and we find them close to MoIsw2 binding motifs
693 (**Table 1, Fig. 5**). The *MoISW2* DNA binding sequences (the ChIPseq
694 sequences) also contained palindromic DNA motifs characteristic of the
695 identified TEs (Bao et al. 2017) (**Fig. 4**). A palindromic DNA motif gives
696 genetic instability to the genome at the site of the motif (Ganapathiraju et al.

697 2020; Svetec Miklenić and Svetec 2021). Stress, virulence, and stress-related
698 genes are in *V. dahliae* (Faino et al. 2016) as well as in *M. oryzae,* are also
699 linked to transposable elements (Yoshida et al. 2016) and we see this in our
700 study as well (**Fig. 6, 7A, 8-10**).

701 Different mutation rates or mutation bias of genes have recently been
702 described as a new concept for the plant *Arabidopsis thaliana* (Monroe et al.
703 2022). Genes with higher mutation rates are involved in biotic and abiotic
704 interactions. The gene found with the highest mutation rate was a gene responding
705 to chitin, which is present in symbiotic (pathogenic and nonpathogenic) fungi and
706 insects (Monroe et al. 2022). Transposable element activity seems important in
707 fungal speciation (Faino et al. 2016) and tends to accumulate in genomes and
708 expand the genome with repetitive sequences (Fijarczyk et al. 2022; Feurtey et al.
709 2023) unless there is some evolutionary constraint against such expansion
710 (Kremer et al. 2020; Fijarczyk et al. 2022). Phosphorous availability is a possible
711 constraint (Ågren et al. 2012) since a considerable amount of the cell phosphorous,
712 especially, is bound up in DNA and not available for other purposes (Berdalet et
713 al. 1994). Fungal plant parasites can get phosphorous directly from their plant
714 hosts by degrading the plant tissue and are not so restricted by limited resources
715 in the soil (Ågren et al. 2012). Thus plant parasitic fungi should be expected to
716 have more retrotransposons to adapt better to plant resistance and thus have
717 relatively large genomes. That is precisely what they have (Fijarczyk et al. 2022;
718 Feurtey et al. 2023). Endophytic fungi that have to coexist with their host in their

719 life cycle, and thus have to compete with the host for phosphorous, should, in
720 consequence, have smaller genomes, as they also seem to have (Fijarczyk et al.
721 2022).

722 Our results show changes in occurrence and regulation of the
723 avirulence genes between two *M. oryzae* strains with different
724 pathogenicity to different rice cultivars (**Table 1**). In addition, we did not
725 detect any expression for some putative avirulence genes close to the
726 MoIsw2 DNA binding sites, suggesting that those genes may be potential
727 pseudogenes in these strains. That might indicate a retrotransposon-aided
728 genetic evolution of inherited epigenetic changes to regulation in reactions
729 to the environment (resistance of the plant cultivar) as has been indicated
730 for *V. dahliae* (Faino et al. 2016). Such regulation can become genetically
731 fixed, first through loss of possible regulation (making downregulated
732 genes into pseudogenes), and much later complete gene loss or change of
733 the potential pseudogenes so they cannot be easily recognized as genes, is
734 a mechanism that could result in a "biased" faster evolution (Chadha and
735 Sharma 2014). Most of the potential pseudogenes (not expressed under any
736 conditions reported in this paper) were close to the MoIsw2 DNA binding
737 sites with palindromic motifs supporting this hypothesis for a mechanism
738 involving MoIsw2 activity in creating pseudogenes and complete removal
739 of genes by making them unrecognizable as genes through mutations. A
740 prerequisite for this to happen is that the ecological niche does not change

741 as fast as it can for a plant pathogen because of efforts of resistance
742 breeding of susceptible plant cultivars. These efforts can then reactivate the
743 silenced genes by TE repositioning to chromosome areas with changed
744 MoIsw2 activity.

745 Our results further indicate that *MoISW2* regulates a switch between
746 fast glycolytic growth with fast DNA synthesis and slower but nutrient-
747 efficient aerobic stress-characterized growth with less DNA synthesis,
748 coping with abiotic and biotic stresses or, in other words, niche fitness. The
749 loss of *ISW2* function in a unicellular Eukaryote or the early stages of
750 fungal growth from a spore should make the fungus unfit for survival in a
751 natural environment and become more dependent on aerobic fermentation
752 for ATP synthesis that is not substrate efficient although generates ATP at
753 a very high rate although inefficient (Pfeiffer and Morley 2014; Desousa et al.
754 2023). However, a limitation for eukaryotic cells to only aerobic
755 fermentation generally leads to uncontrolled cell growth and oncogenesis
756 in a long-lived multicellular organism (Desousa et al. 2023), as ATP and
757 fermentable nutrients can be received from surrounding cells and other
758 tissues through the blood circulation. Thus, mutations of the genes
759 *SMARKA2* or *SMARKA4* that encode Brm and Brg1 proteins that are
760 orthologues of fungal Swi2/Snf2 can cause cancer (Reisman et al. 2009;
761 Mittal and Roberts 2020; Li et al. 2021).

762 On the other hand, a general shift to aerobic glycolysis and a fast
763 upregulation (within a few hours) of innate immunity-related genes and their
764 ATP-dependent translation is associated with tissue inflammation. Such fast de-
765 novo protein synthesis is characteristic of fast defence against microbes needing
766 rapid translational responses and has been shown for *Fusarium graminearum* but
767 is general for eukaryotes (Ipcho et al. 2016). Such fast upregulated plant innate
768 immune responses can be inhibited by fungal-derived immune system inhibitors
769 acting on translation like trichothecenes the fungus (Toyotome and Kamei 2021),
770 most likely to attenuate immune responses in the plants it infects. In line with a
771 fungal innate immunity scenario (Ipcho et al. 2016), genes involved in RNA
772 synthesis and RNA processing were found to be upregulated in the *ΔMoisw2*
773 mutant (**Fig. 3C**).
774

775 **Is retrotransposon shifting *MoISW2* binding creating and directing the**
776 **mutation bias by adapting the fungus to new challenges?**

777 *MoISW2* is likely an important player in a mechanism aiding both mutation
778 bias and adaptation to new circumstances whose combined activities lead
779 to two-speed evolution of the fungal genome (Faino et al. 2016) a slow
780 random evolution and a fast more directed by adaptations. The faster speed
781 evolution can be named natural adaptation-directed fast evolution (NADFE), a
782 new concept that is similar to artificial adaptation-directed fast evolution that can
783 be performed in a laboratory (Packer and Liu 2015). The suggested mechanism is

784 the following: As transposon DNA containing MoIsw2 palindromic DNA binding
785 sites seems necessary for MoIsw2 activity, stress-activated transposon activity,
786 known for creating genomic instability, can together with the MoIsw2 activity
787 create a new adaptive regulatory landscape (Chadha and Sharma 2014) that can
788 be stabilized relatively quickly and lead to mutation bias (Monroe et al. 2022). In
789 addition, the Isw2 stabilized expression landscape further stabilized by later
790 mutations could be the mechanism sought after for a Lamarckian-Darwinian
791 synthesis. This mechanism can explain the fast evolution of new traits requiring
792 many combined mutations that cannot be reconciled within Darwinian strict
793 random evolution creating variation together with sexual recombination and
794 natural selection to cause both the observed direction and the needed speed of
795 evolution of specific traits when new niches become available, or there are drastic
796 niche changes (Bard 2011). The chance of multiple mutations that only together
797 can become positive is theoretically much more likely to happen with NADFE
798 first creating a mutation bias (Monroe et al. 2022).
799

800 **Perspectives for Future Research**

801 *Evolution of the plant-pathogen interaction:* The effect of exposing *M.*
802 *oryzae* strains to different MoIsw2 activities and retrotransposon activities
803 on the rate of genetic adaptation to a shift in rice cultivar is a possible future
804 topic that could be exploited to understand how the pathogen adapts to
805 different resistant cultivars and break plant resistance.

806 *Agrochemicals:* Searching for potential agrochemicals to manipulate
807 MoIsw2 activities on His4 and DNA-binding is tempting since *MoISW2* is
808 crucial for plant pathogenicity. Though MoIsw2's close resemblance to
809 mammalian proteins with the same function indicates that such chemicals
810 are likely negatively affecting orthologue proteins in mammals and might
811 be cancerogenic to humans since even small mutations in *ISW2* orthologues
812 in mammals can cause cancer (Reisman et al. 2009; Mittal and Roberts 2020).
813 ***Histon4:*** Finally, we found 2 *MoHIS4* genes with large differences in DNA
814 sequences (gene duplication many generations ago) predicted to encode for
815 identical proteins but differently regulated and it seems like *M. oryzae*
816 needs both genes (**Fig. 2**). This fact is of interest since His4 proteins in
817 nucleosomes is what MoIsw2 is supposed to interact with (Tsukiyama et al.
818 1999), and *HIS4*s are examples of genes with the highest degree of purifying
819 evolution (Piontkivska et al. 2002). We have thus started new research into
820 the roles and regulation of these two *MoHIS4* genes and how their
821 regulations shift with growth conditions. Their predicted identical amino
822 acid sequences indicate that they are evolutionarily constrained to differ
823 only by synonymous mutations.
824 *Gene expression variability:* The most interesting genes for biotic and
825 abiotic interactions are also the genes with the highest variability between
826 experiments (VarR) creating problems when proving the effects gene
827 deletions. The common practice of only using 3 replicates for measuring

828 effects on genes (like deletions) is probably not enough and we might need
829 to increase the number of replicates to 5 for the gene expression in the wild
830 type. If we do that we can either statistically prove what type of distribution
831 there is and use that or better use non-parametric methods not assuming the
832 distribution. Strict normal or more correctly lognormal distribution
833 (negative expression is not possible!) may also be true mainly for
834 housekeeping genes.
835
836 **Consequences of MoIsw2 functions that are positive for the fungus's ability**
837 **to stay pathogenic:** 1. The MoIsw2 function will result in adaptive silencing of
838 virulence/avirulence genes without gene loss due to mutations of the actual DNA
839 nucleotides. In other words, virulence genes are not quickly lost from the adapted
840 strains but can be "called upon again" if the available hosts change their resistance
841 in the classical gene-for-gene scenario (Flor 1956). 2. Adaptive silencing of
842 virulence genes is often found close to transposable elements (Menardo et al. 2017)
843 and that will lead to biased fast gene evolution of especially genes involved in
844 biotic interaction (Monroe et al. 2022) and in the gene-for-gene concept and is a
845 possible mechanism behind the speedy appearance of virulent pathogen strains
846 capable of attacking newly developed resistant plant varieties (Palloix et al. 2009;
847 Menardo et al. 2017).
848
849

850

851

852 **Materials and Methods**

853

854 **Fungal strains and media**

855 *Magnaporthe oryzae* B. Couch anamorph of the teleomorph *Pyricularia oryzae*
856 Cavara was used for this research. As background strain, we used Ku80
857 (generated from the WT strain 70-15) to minimize random integration events
858 when transformed (Villalba et al. 2008). The susceptible Indica rice (cv. CO-39)
859 and barley (cv. Golden Promise) used for the fungal pathogenicity tests were from
860 the seed bank of our laboratory. For both ChIP-seq and RNAseq, the strains used
861 were grown and harvested similarly.

862

863 **Knockouts, complementations, and verifications**

864 The *MoISW2* is a *MYB* gene and *MYB* gene deletion vectors were constructed in
865 the plasmid pBS-HYG by inserting 1 kb up- and down-stream fragments of the
866 target gene's coding region as flanking regions of the HPH (hygromycin
867 phosphotransferase) gene (Li et al. 2012). No less than 2 μg of the deletion vector
868 DNA of the target gene was introduced to Ku80 protoplasts, and transformants
869 were selected for hygromycin resistance to perform gene deletion transformations.
870 Southern blotting was conducted to confirm the correct deletion using the
871 digoxigenin (DIG) high prime DNA labelling and detection starter Kit I

872 (11745832910 Roche Germany). The *MYB* gene complementation vectors were
873 constructed by cloning the entire length of the target gene with the native promoter
874 region (about 1.5 kb) to the pCB1532 plasmid. When making the
875 complementation vector, GFP was linked to the C-terminal of the target genes to
876 study the sub-cellar localization of Myb proteins. The constructed vector DNA
877 was introduced into the mutation protoplast for gene complementation, and
878 resulting transformants were screened using 50 μg/ml chlorimuron-ethyl to select
879 successful complementation strains. Detailed fungal protoplast preparation and
880 transformation methods have been described previously (Li et al. 2012). All
881 primers needed for the knockout and complementation are listed (**Table S1**). The
882 sub-cellar localization of Myb proteins was observed by confocal microscopy
883 (Nikon A1). GFP and RFP excitation wavelengths were 488 nm and 561 nm,
884 respectively.
885

886 **Colony growth and infection phenotype measurements**

887 Vegetative growth was tested by measuring the colony diameter after ten days of
888 growth in 9 cm Petri dishes at 25℃ under 12h-to-12h light and dark periods.
889 Conidia production was evaluated by flooding the 12-day-old colony with double
890 distilled water, filtering out the mycelia with gauze, and counting the conidia
891 using a hemacytometer. The conidiophore induction assay was performed by
892 excising one thin agar block from the fungal colony and then incubating it in a
893 sealed chamber for 24 h with constant light (Li, Yan, et al. 2010). Mycelia

894 appressoria was induced by placing a suspension of mycelial fragments on a
895 hydrophobic surface in a humid environment at 25℃ for 24h. The pathogenicity
896 assay on rice was performed by spraying 5 ml conidial suspension (5×10^4
897 spores/ml) on 15-day-old plants (Y. Li et al. 2019). The inoculated plants were
898 kept in a sealed chamber with a 90% relative humidity at 25℃ for 24 h before the
899 inoculated plants were removed from the chamber to allow disease symptoms to
900 develop for 4-5 days. The pathogenicity assay on excised barley and rice leaves
901 was performed by cutting a small block from the agar culture of the fungus and
902 placing it on excised leaves for five days in a moist chamber for disease
903 development (Li, Liang, et al. 2010). Sexual reproduction was tested by crossing
904 the tested strain with the sexually compatible strain TH3 on OM plates and then
905 incubating at 19℃ for 30 days with continuous light. The perithecia and clavate
906 asci were photographed in a microscope equipped with a camera (OLYMPUS
907 BX51).
908
909 **Biomass production for ChIPseq and RNAseq**
910 For ChIP-seq, the complemented strain, MoIsw2-GFP and the strain Ku80 were
911 used, and for RNAseq *ΔMoisw2* and *Ku80* were used. The strains were grown on
912 Complete medium 2 (CM2) all are quantities L^-: 20X Mineral salts solution 50mL,
913 1000X Trace element solution 1mL, 1000X vitamin solution 1mL, D-glucose 10g,
914 peptone 2g, casamino acid 1g, yeast extract 1g, pH 6.5. For agar medium add 15g

915 agar. Supplemented with 20×Mineral salts solution (per 1000mL): NaNO3 120g，
916 KCl 10.4g， MgSO4 7H2O 10.4g， KH2PO4 30.4g and with 1000X Vitamin
917 solution (per 100mL): Biotin 0.01g, Pyridoxin 0.01g, Thiamine 0.01g, Riboflavin
918 0.01g, PABA (p-aminobenzoic acid) 0.01g, Nicotinic acid 0.01g and 1000X
919 Trace element (per 100mL): $ZnSO_4$ $7H_2O$ 2.2g, H_3BO_3 1.1g $MnCl_2$ $4H_2O$ 0.5g,
920 $FeSO_4$ $7H_2O$ 0.5g $CoCl_2$ $6H_2O$ 0.17g, $CuSO_4$ $5H_2O$, Na_2MoO_4 $5H_2O$ 0.15g,
921 EDTA 4Na 5g. The plates were incubated for 4-5 days at 28ºC with alternating
922 light-dark cycles (12/12). Mycelial disks (15-20) were punched out at the colony's
923 edge using a 5 mm diameter cork puncher. The disks were transferred to 100 ml
924 CM2 liquid medium and shake cultured for another 48h (160 RPM, Constant
925 temperature culture oscillator, ZHWY-2102C, Shanghai Zhicheng Analytical
926 Instrument Manufacturing Co., Ltd.). The obtained biomass was filtered using
927 Miracloth, frozen in liquid nitrogen, and sent on dry ice to the company
928 performing the RNAseq.
929
930 **ChIP-seq and RNA-seq**
931 Both these techniques were carried out by the company Wuhan IGENEBOOK
932 Biotechnology Co., Ltd, China, according to their method descriptions
933 **(Supplemental Company Methods file**). The last steps about finding motifs and
934 enriched gene classes were carried out differently and are described in this paper.
935 These steps not used are marked in the two Supplementary method files.

936

937 **Method for calculating VarR and DelR in the RNAseq data.**

938 We calculated the variability in gene expression for each gene for all the
939 downloaded experimental datasets in the following way. First, we checked that
940 the quality of the data was ok. We have previously found for our own
941 transcriptomic data that a dataset is ok if expressions of genes are rank-ordered
942 then the log log expression of log expression level against the log-rank order
943 should be a smooth downward slightly curved line without big gaps. Also, to be
944 able to compare different sets of data from different experiments the total
945 expression of all genes summed should be similar for all datasets. Next, we
946 calculated the maximum variation between experiments in the following way.
947 The maximum expression value and the minimum expression value for each
948 gene across the 55 transcriptomes were found. Next, we calculated the average
949 expression for the same data. Finally, we calculated the ratio of maximum
950 expression minus minimum expression divided by the average expression to
951 arrive at the variation in expression across all experiments for each gene (VarR).
952 In this way any regulation up or down is treated in the same way as access for
953 TFs and repressors to the DNA should be treated equally. Finally comes the
954 problem that some genes had expression values lower than the threshold for
955 detecting them at all (0-values). For these data, we assumed that the expression
956 where at the threshold value instead of 0 and set the expression to that value. In

957 that way, we could include that data without overestimating the VarR for that
958 gene.
959
960 The effect of the *MoISW2* mutation (DelR) was estimated in the following way
961 to make it comparable with VarR: For each gene, we calculated the 2Log ratio
962 of the expression in the mutant divided by the expression in the background.
963 That results in both negative and positive values. Then these values were
964 squared to arrive at only positive values in a similar way as is done with the least
965 square method for curve fitting to arrive at a better estimate of the deviation
966 from the slope. There were very few genes with no detectable expression so no
967 need for handling zero values more than excluding them.
968
969 Note that in this paper, we focus on the expression variation of all genes along
970 the chromosomes. Thus, it is the overall pattern that is important and not the
971 values for a single gene. In none of the methods above we used any method for
972 excluding a gene from the analysis based on an arbitrary threshold of 2 times up
973 or down or any other statistically significant threshold for genes. In
974 consequence, the calculated values for a single gene cannot and should not be
975 relied upon even if a general increased regulation of many adjacent genes has
976 reliability.
977
978

979 **Additional software and add-ins for MS Excel**

980 ***Addins for MS Excel:*** The **Fisher Exact** add-in for MS Excel was downloaded
981 from http://www.obertfamily.com/software/fisherexact.html. The **Excel solver**
982 was used to fit non-standard equations to data. The Solver is usually part of MS
983 Excel but must be activated in settings.

984 **Freeware:** We used the freeware PAST A simple-to-use but powerful freeware
985 program is available from the University of Oslo, Natural History Museum
986 **https://www.nhm.uio.no/english/research/infrastructure/past/** (Hammer et al.
987 2001) version 4.08 (released November 2021). We mainly used the software for
988 Reduced Major Axis (RMA) regression analysis to handle errors in both the x and
989 y variables. For simplicity, the data was handled and entered in MS Excel and
990 then copy-pasted into PAST for analysis. The resulting plots were exported from
991 PAST as SVG vector graphic files to be later translated into other vector graphic
992 file formats.

993 **Websites used for analyses and getting necessary additional data**

994 **NCBI**: **https://www.ncbi.nlm.nih.gov/** (sequence downloads, blasts, annotations
995 including domain annotations)

996 **BROAD**: **ftp://ftp.broadinstitute.org** (download of gene order on supercontigs
997 for the Guy11 strain, 1000 upstream DNA sequences for use in MEME)

998 **MEME: https://meme-suite.org/meme/** (use of MEME and FIMO). (Bailey et
999 al. 2015).

1000 See the supplemental file for MEME settings and complete results (Supplemental
1001 Data 2). MEME motif 2 was the one with the most hits and was investigated in
1002 detail. This motif2 was used for TOMTOM by using the direct link to TOMTOM
1003 using the link from the MEME result, for results see the supplemental file
1004 (Supplemental Data 3).

1005 **FungiFun2 https://elbe.hki-jena.de/fungifun/fungifun.php** (Priebe et al. 2015)
1006 Species**:** *Magnaporthe grisea* 70-15 (synonym for *M. oryzae* 70-15).
1007 Classification ontology: FunCat (contains more relevant categories for fungal
1008 plant pathogens than Kegg or GO)
1009 Input IDs: For *M. oryzae* 70-15 the MGG_ codes has to be used.
1010 Advanced settings used**:** Significance level; 0.05. Significance test; Fisher's exact
1011 test. Test for; Enrichment or Depletion. Adjustment method; No adjustment.
1012 Annotation type, Select also indirectly annotated categories.
1013 These settings using "No adjustment" were used since the purpose was not to get
1014 super reliable enriched or depleted categories but to compare several FungiFun
1015 runs with different Gene ID sets.

1016 **antiSMASH**

1017 The complete DNA sequence of *M. oryzae* 70-15 was downloaded from BROAD.
1018 That was then submitted to antiSMASH (Blin et al. 2021) fungal version
1019 **https://fungismash.secondarymetabolites.org/#!/start** and run with default
1020 parameter settings to find the core genes predicted to be involved in producing
1021 secondary metabolites.

Acknowledgements

This work was supported by grants from the Fujian Provincial Science and Technology Key Project (2022NZ030014) Fujian Natural Science Foundation project (2022J01125).

1029 References

1030 Ågren GI, Wetterstedt JÅM, Billberger MFK. 2012. Nutrient limitation on terrestrial plant
1031 growth – modeling the interaction between nitrogen and phosphorus. *New Phytologist*
1032 194:953–960.

1033 Allan AC, Espley RV. 2018. MYBs Drive Novel Consumer Traits in Fruits and Vegetables.
1034 *Trends in Plant Science* 23:693–705.

1035 Ambawat S, Sharma P, Yadav NR, Yadav RC. 2013. MYB Transcription Factor Genes as
1036 Regulators for Plant Responses: An Overview. *Physiol Mol Biol Plants* 19:307–321.

1037 Andrew M, Barua R, Short SM, Kohn LM. 2012. Evidence for a Common Toolbox Based on
1038 Necrotrophy in a Fungal Lineage Spanning Necrotrophs, Biotrophs, Endophytes, Host
1039 Generalists and Specialists.Stajich JE, editor. *PLoS ONE* 7:e29943.

1040 Bailey TL, Johnson J, Grant CE, Noble WS. 2015. The MEME Suite. *Nucleic Acids Res*
1041 43:W39–W49.

1042 Baldoni E, Genga A, Cominelli E. 2015. Plant MYB Transcription Factors: Their Role in
1043 Drought Response Mechanisms. *Int. J. Mol. Sci.*:41.

1044 Bao J, Chen M, Zhong Z, Tang W, Lin L, Zhang X, Jiang H, Zhang D, Miao C, Tang H, et al.
1045 2017. PacBio Sequencing Reveals Transposable Elements as a Key Contributor to
1046 Genomic Plasticity and Virulence Variation in Magnaporthe oryzae. *Molecular Plant*
1047 10:1465–1468.

1048 Bard JB. 2011. The next evolutionary synthesis: from Lamarck and Darwin to genomic
1049 variation and systems biology. *Cell Commun Signal* 9:30.

1050 Berdalet E, Latasa M, Estrada M. 1994. Effects of nitrogen and phosphorus starvation on
1051 nucleic acid and protein content of *Heterocapsa* sp. *Journal of Plankton Research*
1052 16:303–316.

1053 Blin K, Shaw S, Kloosterman AM, Charlop-Powers Z, van Wezel GP, Medema MH, Weber
1054 T. 2021. antiSMASH 6.0: improving cluster detection and comparison capabilities.
1055 *Nucleic Acids Research* 49:W29–W35.

1056 Bourras S, McNally KE, Müller MC, Wicker T, Keller B. 2016. Avirulence Genes in Cereal
1057 Powdery Mildews: The Gene-for-Gene Hypothesis 2.0. *Front. Plant Sci.* [Internet] 7.
1058 Available from: http://journal.frontiersin.org/article/10.3389/fpls.2016.00241

1059 Cao Y, Chen J, Xie X, Liu S, Jiang Y, Pei M, Wu Q, Qi P, Du L, Peng B, et al. 2022.
1060 Characterization of two infection-induced transcription factors of *Magnaporthe oryzae*
1061 reveals their roles in regulating early infection and effector expression. *Molecular*
1062 *Plant Pathology* 23:1200–1213.

1063 Cao Y, Li K, Li Y, Zhao X, Wang L. 2020. MYB Transcription Factors as Regulators of
1064 Secondary Metabolism in Plants. *Biology* 9:61.

1065 Chadha S, Sharma M. 2014. Transposable Elements as Stress Adaptive Capacitors Induce
1066 Genomic Instability in Fungal Pathogen Magnaporthe oryzae.Han K-H, editor. *PLoS*
1067 *ONE* 9:e94415.

1068 Cheetham SW, Faulkner GJ, Dinger ME. 2020. Overcoming challenges and dogmas to
1069 understand the functions of pseudogenes. *Nat Rev Genet* 21:191–201.

1070 Chowdhury S, Basu A, Kundu S. 2017. Biotrophy-necrotrophy switch in pathogen evoke
1071 differential response in resistant and susceptible sesame involving multiple signaling
1072 pathways at different phases. *Sci Rep* 7:17251.

1073 Collemare J, Pianfetti M, Houlle A, Morin D, Camborde L, Gagey M, Barbisan C, Fudal I,
1074 Lebrun M, Böhnert HU. 2008. *Magnaporthe grisea* avirulence gene *ACE1* belongs to
1075 an infection-specific gene cluster involved in secondary metabolism. *New Phytologist*
1076 179:196–208.

1077 Cutter AR, Hayes JJ. 2015. A brief review of nucleosome structure. *FEBS Letters* 589:2914–
1078 2922.

1079 Dang W, Sutphin GL, Dorsey JA, Otte GL, Cao K, Perry RM, Wanat JJ, Saviolaki D,
1080 Murakami CJ, Tsuchiyama S, et al. 2014. Inactivation of Yeast Isw2 Chromatin
1081 Remodeling Enzyme Mimics Longevity Effect of Calorie Restriction via Induction of
1082 Genotoxic Stress Response. *Cell Metabolism* 19:952–966.

1083 Desousa BR, Kim KK, Jones AE, Ball AB, Hsieh WY, Swain P, Morrow DH, Brownstein
1084 AJ, Ferrick DA, Shirihai OS, et al. 2023. Calculation of ATP production rates using
1085 the Seahorse XF Analyzer. *EMBO Reports*:e56380.

1086 Dioh W, Tharreau D, Notteghem JL, Orbach M, Lebrun M-H. 2000. Mapping of Avirulence
1087 Genes in the Rice Blast Fungus, *Magnaporthe grisea* , with RFLP and RAPD
1088 Markers. *MPMI* 13:217–227.

1089 Dong Y, Li Y, Zhao M, Jing M, Liu X, Liu M, Guo X, Zhang X, Chen Y, Liu Yongfeng, et
1090 al. 2015. Global Genome and Transcriptome Analyses of Magnaporthe oryzae
1091 Epidemic Isolate 98-06 Uncover Novel Effectors and Pathogenicity-Related Genes,
1092 Revealing Gene Gain and Lose Dynamics in Genome Evolution.Lin X, editor. *PLoS*
1093 *Pathog* 11:e1004801.

1094 Donovan DA, Crandall JG, Truong VN, Vaaler AL, Bailey TB, Dinwiddie D, Banks OG,
1095 McKnight LE, McKnight JN. 2021. Basis of specificity for a conserved and
1096 promiscuous chromatin remodeling protein. *eLife* 10:e64061.

1097 Du H, Zhang L, Liu L, Tang X-F, Yang W-J, Wu Y-M, Huang Y-B, Tang Y-X. 2009.
1098 Biochemical and Molecular Characterization of Plant MYB Transcription Factor
1099 Family. *Biochemistry Moscow* 74:1–11.

1100 Dubos C, Stracke R, Grotewold E, Weisshaar B, Martin C, Lepiniec L. 2010. MYB
1101 Transcription Factors in *Arabidopsis*. *Trends in Plant Science* 15:573–581.

1102 Erdel F, Rippe K. 2011. Binding kinetics of human ISWI chromatin-remodelers to DNA
1103 repair sites elucidate their target location mechanism. *Nucleus* 2:105–112.

1104 Erdel F, Schubert T, Marth C, Längst G, Rippe K. 2010. Human ISWI chromatin-remodeling
1105 complexes sample nucleosomes via transient binding reactions and become
1106 immobilized at active sites. *Proc. Natl. Acad. Sci. U.S.A.* 107:19873–19878.

1107 Faino L, Seidl MF, Shi-Kunne X, Pauper M, Van Den Berg GCM, Wittenberg AHJ, Thomma
1108 BPHJ. 2016. Transposons passively and actively contribute to evolution of the two-
1109 speed genome of a fungal pathogen. *Genome Res.* 26:1091–1100.

1110 Fazzio TG, Gelbart ME, Tsukiyama T. 2005. Two Distinct Mechanisms of Chromatin
1111 Interaction by the Isw2 Chromatin Remodeling Complex In Vivo. *Mol Cell Biol*
1112 25:9165–9174.

1113 Feurtey A, Lorrain C, McDonald MC, Milgate A, Solomon PS, Warren R, Puccetti G, Scalliet
1114 G, Torriani SFF, Gout L, et al. 2023. A thousand-genome panel retraces the global
1115 spread and adaptation of a major fungal crop pathogen. *Nat Commun* 14:1059.

1116 Fijarczyk A, Hessenauer P, Hamelin RC, Landry CR. 2022. Lifestyles shape genome size and
1117 gene content in fungal pathogens. Available from:
1118 http://biorxiv.org/lookup/doi/10.1101/2022.08.24.505148

1119 Flor HH. 1956. The Complementary Genic Systems in Flax and Flax Rust. In: Advances in
1120 Genetics. Vol. 8. Elsevier. p. 29–54. Available from:
1121 https://linkinghub.elsevier.com/retrieve/pii/S0065266008604988

1122 Ganapathiraju MK, Subramanian S, Chaparala S, Karunakaran KB. 2020. A reference catalog
1123 of DNA palindromes in the human genome and their variations in 1000 Genomes.
1124 *Hum Genome Var* 7:40.

1125 Hada A, Hota SK, Luo J, Lin Y, Kale S, Shaytan AK, Bhardwaj SK, Persinger J, Ranish J,
1126 Panchenko AR, et al. 2019. Histone Octamer Structure Is Altered Early in ISW2 ATP-
1127 Dependent Nucleosome Remodeling. *Cell Reports* 28:282-294.e6.

1128 Hammer O, Harper DAT, Ryan PD. 2001. PAST: Paleontological Statistics Software Package
1129 for Education and Data Analysis. 4:9.

1130 van Holde KE. 1989. Chromatin. New York, NY: Springer New York Available from:
1131 http://link.springer.com/10.1007/978-1-4612-3490-6

1132 Hopfner K-P, Gerhold C-B, Lakomek K, Wollmann P. 2012. Swi2/Snf2 remodelers: hybrid
1133 views on hybrid molecular machines. *Current Opinion in Structural Biology* 22:225–
1134 233.

1135 Hota SK, Bartholomew B. 2011. Diversity of operation in ATP-dependent chromatin
1136 remodelers. *Biochimica et Biophysica Acta (BBA) - Gene Regulatory Mechanisms*
1137 1809:476–487.

1138 Huang L, Li X, Dong L, Wang B, Pan L. 2021. Profiling of chromatin accessibility identifies
1139 transcription factor binding sites across the genome of Aspergillus species. *BMC Biol*
1140 19:189.

1141 Ipcho S, Sundelin T, Erbs G, Kistler HC, Newman M-A, Olsson S. 2016. Fungal innate
1142 immunity induced by bacterial microbe-associated molecular patterns (MAMPs). *G3*
1143 6:1585–1595.

1144 Jones JDG, Dangl JL. 2006. The plant immune system. *Nature* 444:323–329.

1145 Josefsen L, Droce A, Sondergaard TE, Sørensen JL, Bormann J, Schäfer W, Giese H, Olsson
1146 S. 2012. Autophagy provides nutrients for nonassimilating fungal structures and is
1147 necessary for plant colonization but not for infection in the necrotrophic plant
1148 pathogen Fusarium graminearum. *Autophagy* 8:326–337.

1149 Kagalwala MN, Glaus BJ, Dang W, Zofall M, Bartholomew B. 2004. Topography of the
1150 ISW2–nucleosome complex: insights into nucleosome spacing and chromatin
1151 remodeling. *EMBO J* 23:2092–2104.

1152 Kim Y, Kim H, Son H, Choi GJ, Kim J-C, Lee Y-W. 2014. MYT3, A Myb-Like
1153 Transcription Factor, Affects Fungal Development and Pathogenicity of Fusarium
1154 graminearum.Yu J-H, editor. *PLoS ONE* 9:e94359.

1155 Klevecz RR, Bolen J, Forrest G, Murray DB. 2004. A genomewide oscillation in transcription
1156 gates DNA replication and cell cycle. *Proceedings of the National Academy of*
1157 *Sciences* 101:1200–1205.

1158 Kou Y, Qiu J, Tao Z. 2019. Every Coin Has Two Sides: Reactive Oxygen Species during
1159 Rice–*Magnaporthe oryzae* Interaction. *IJMS* 20:1191.

1160 Kremer SC, Linquist S, Saylor B, Elliott TA, Gregory TR, Cottenie K. 2020. Transposable
1161 element persistence via potential genome-level ecosystem engineering. *BMC*
1162 *Genomics* 21:367.

1163 Li H, Lu J, Liu X, Xhang L, Lin F. 2012. Vector Building and Usage for Gene Knockout,
1164 Protein Expression and Fluorescent Fusion Protein in The Rice Blast Fungus. *Journal*
1165 *of Agricultural Biotechnology* 20:94–104.

1166 Li J, Han G, Sun C, Sui N. 2019. Research Advances of MYB Transcription Factors in Plant
1167 Stress Resistance and Breeding. *Plant Signaling & Behavior* 14:1613131.

1168 Li Y, Gong H, Wang P, Zhu Y, Peng H, Cui Y, Li H, Liu J, Wang Z. 2021. The emerging role
1169 of ISWI chromatin remodeling complexes in cancer. *J Exp Clin Cancer Res* 40:346.

1170 Li Y, Liang S, Yan X, Wang H, Li D, Soanes DM, Talbot NJ, Wang Zonghua, Wang
1171 Zhengyi. 2010. Characterization of *MoLDB1* Required for Vegetative Growth,
1172 Infection-Related Morphogenesis, and Pathogenicity in the Rice Blast Fungus
1173 *Magnaporthe oryzae*. *MPMI* 23:1260–1274.

1174 Li Y, Yan X, Wang H, Liang S, Ma W-B, Fang M-Y, Talbot NJ, Wang Z-Y. 2010. MoRic8 Is
1175 a Novel Component of G-Protein Signaling During Plant Infection by the Rice Blast
1176 Fungus *Magnaporthe oryzae*. *MPMI* 23:317–331.

1177 Li Y, Yue X, Que Y, Yan X, Ma Z, Talbot NJ, Wang Z. 2014. Characterisation of Four LIM
1178 Protein-Encoding Genes Involved in Infection-Related Development and

1179 Pathogenicity by the Rice Blast Fungus Magnaporthe oryzae.Xue C, editor. *PLoS*
1180 *ONE* 9:e88246.

1181 Li Y, Zheng X, Pei M, Chen M, Zhang S, Liang C, Gao L, Huang P, Olsson S. 2024.
1182 Functional Analysis of MoMyb13, a Myb Transcription Factor Involved in Regulating
1183 Growth, Conidiation, Hydrophobicity, and Pathogenicity of Magnaporthe oryzae.
1184 *Agronomy* 14:251.

1185 Li Y, Zheng X, Zhu M, Chen M, Zhang S, He F, Chen X, Lv J, Pei M, Zhang Ye, et al. 2019.
1186 MoIVD-Mediated Leucine Catabolism Is Required for Vegetative Growth,
1187 Conidiation and Full Virulence of the Rice Blast Fungus Magnaporthe oryzae. *Front.*
1188 *Microbiol.* 10:444.

1189 Lin Y, Son H, Lee J, Min K, Choi GJ, Kim J-C, Lee Y-W. 2011. A Putative Transcription
1190 Factor MYT1 Is Required for Female Fertility in the Ascomycete Gibberella zeae.Yu
1191 J-H, editor. *PLoS ONE* 6:e25586.

1192 Lin Y, Son H, Min K, Lee J, Choi GJ, Kim J-C, Lee Y-W. 2012. A Putative Transcription
1193 Factor MYT2 Regulates Perithecium Size in the Ascomycete Gibberella zeae.Yu J-H,
1194 editor. *PLoS ONE* 7:e37859.

1195 Linheiro RS, Bergman CM. 2008. Testing the palindromic target site model for DNA
1196 transposon insertion using the Drosophila melanogaster P-element. *Nucleic Acids*
1197 *Research* 36:6199–6208.

1198 Liu J, Osbourn A, Ma P. 2015. MYB Transcription Factors as Regulators of Phenylpropanoid
1199 Metabolism in Plants. *Molecular Plant* 8:689–708.

1200 Ma D, Constabel CP. 2019. MYB Repressors as Regulators of Phenylpropanoid Metabolism
1201 in Plants. *Trends in Plant Science* 24:275–289.

1202 Machné R, Murray DB. 2012. The Yin and Yang of Yeast Transcription: Elements of a
1203 Global Feedback System between Metabolism and Chromatin.Saks V, editor. *PLoS*
1204 *ONE* 7:e37906.

1205 Mateos L, Jiménez A, Revuelta JL, Santos MA. 2006. Purine Biosynthesis, Riboflavin
1206 Production, and Trophic-Phase Span Are Controlled by a Myb-Related Transcription
1207 Factor in the Fungus *Ashbya gossypii*. *Appl Environ Microbiol* 72:5052–5060.

1208 Matheis S, Yemelin A, Scheps D, Andresen K, Jacob S, Thines E, Foster AJ. 2017. Functions
1209 of the Magnaporthe oryzae Flb3p and Flb4p transcription factors in the regulation of
1210 conidiation. *Microbiological Research* 196:106–117.

1211 Menardo F, Praz CR, Wicker T, Keller B. 2017. Rapid turnover of effectors in grass powdery
1212 mildew (Blumeria graminis). *BMC Evol Biol* 17:223.

1213 Mitra P. 2018. Transcription Regulation of MYB: a Potential and Novel Therapeutic Target in
1214 Cancer. *Ann. Transl. Med* 6:443–443.

1215 Mittal P, Roberts CWM. 2020. The SWI/SNF complex in cancer — biology, biomarkers and
1216 therapy. *Nat Rev Clin Oncol* 17:435–448.

1217 Monroe JG, Srikant T, Carbonell-Bejerano P, Becker C, Lensink M, Exposito-Alonso M,
1218 Klein M, Hildebrandt J, Neumann M, Kliebenstein D, et al. 2022. Mutation bias
1219 reflects natural selection in Arabidopsis thaliana. *Nature* 602:101–105.

1220 Nürnberger T, Brunner F, Kemmerling B, Piater L. 2004. Innate immunity in plants and
1221 animals: striking similarities and obvious differences. *Immunological Reviews*
1222 198:249–266.

1223 Packer MS, Liu DR. 2015. Methods for the directed evolution of proteins. *Nat Rev Genet*
1224 16:379–394.

1225 Palloix A, Ayme V, Moury B. 2009. Durability of plant major resistance genes to pathogens
1226 depends on the genetic background, experimental evidence and consequences for
1227 breeding strategies. *New Phytologist* 183:190–199.

1228 Pattabiraman DR, Gonda TJ. 2013. Role and Potential for Therapeutic targeting of MYB in
1229 Leukemia. *Leukemia* 27:269–277.

1230 Pfeiffer T, Morley A. 2014. An evolutionary perspective on the Crabtree effect. *Front. Mol.*
1231 *Biosci.* [Internet] 1. Available from:
1232 http://journal.frontiersin.org/article/10.3389/fmolb.2014.00017/abstract

1233 Piontkivska H, Rooney AP, Nei M. 2002. Purifying Selection and Birth-and-death Evolution
1234 in the Histone H4 Gene Family. *Molecular Biology and Evolution* 19:689–697.

1235 Priebe S, Kreisel C, Horn F, Guthke R, Linde J. 2015. FungiFun2: a comprehensive online
1236 resource for systematic analysis of gene lists from fungal species. *Bioinformatics*
1237 31:445–446.

1238 Prouse MB, Campbell MM. 2012. The Interaction Between MYB Proteins and their Target
1239 DNA binding Sites. *Biochimica et Biophysica Acta (BBA) - Gene Regulatory*
1240 *Mechanisms* 1819:67–77.

1241 Rajarammohan S. 2021. Redefining Plant-Necrotroph Interactions: The Thin Line Between
1242 Hemibiotrophs and Necrotrophs. *Front. Microbiol.* 12:673518.

1243 Reisman D, Glaros S, Thompson EA. 2009. The SWI/SNF complex and cancer. *Oncogene*
1244 28:1653–1668.

1245 Roy S. 2016. Function of MYB Domain Transcription Factors in Abiotic Stress and
1246 Epigenetic Control of Stress Response in Plant Genome. *Plant Signaling & Behavior*
1247 11:e1117723.

1248 Serrano L, Vazquez BN, Tischfield J. 2013. Chromatin structure, pluripotency and
1249 differentiation. *Exp Biol Med (Maywood)* 238:259–270.

1250 Song Z, Bakeer W, Marshall JW, Yakasai AA, Khalid RM, Collemare J, Skellam E, Tharreau
1251 D, Lebrun M-H, Lazarus CM, et al. 2015. Heterologous expression of the avirulence
1252 gene ACE1 from the fungal rice pathogen Magnaporthe oryzae. *Chem. Sci.* 6:4837–
1253 4845.

1254 Stanton KA, Edger PP, Puzey JR, Kinser T, Cheng P, Vernon DM, Forsthoefel NR, Cooley
1255 AM. 2017. A Whole-Transcriptome Approach to Evaluating Reference Genes for
1256 Quantitative Gene Expression Studies: A Case Study in *Mimulus*. *G3*
1257 *Genes|Genomes|Genetics* 7:1085–1095.

1258 Svetec Miklenić M, Svetec IK. 2021. Palindromes in DNA—A Risk for Genome Stability and
1259 Implications in Cancer. *IJMS* 22:2840.

1260 Toyotome T, Kamei K. 2021. In Vitro Assay of Translation Inhibition by Trichothecenes
1261 Using a Commercially Available System. *Toxins* 13:696.

1262 Tsukiyama T, Palmer J, Landel CC, Shiloach J, Wu C. 1999. Characterization of the Imitation
1263 Switch subfamily of ATP-dependent chromatin-remodeling factors in Saccharomyces
1264 cerevisiae. *Genes & Development* 13:686–697.

1265 Valsecchi I, Sarikaya-Bayram Ö, Wong Sak Hoi J, Muszkieta L, Gibbons J, Prevost M-C,
1266 Mallet A, Krijnse-Locker J, Ibrahim-Granet O, Mouyna I, et al. 2017. MybA, a
1267 transcription factor involved in conidiation and conidial viability of the human
1268 pathogen *Aspergillus fumigatus*: A transcription factor regulating conidiation in
1269 *Aspergillus*. *Molecular Microbiology* 105:880–900.

1270 Verma S, Gazara RK, Verma PK. 2017. Transcription Factor Repertoire of Necrotrophic
1271 Fungal Phytopathogen *Ascochyta rabiei*: Predominance of MYB Transcription Factors
1272 As Potential Regulators of Secretome. *Front. Plant Sci.* 8:1037.

1273 Villalba F, Collemare J, Landraud P, Lambou K, Brozek V, Cirer B, Morin D, Bruel C, Beffa
1274 R, Lebrun M-H. 2008. Improved gene targeting in Magnaporthe grisea by inactivation
1275 of MgKU80 required for non-homologous end joining. *Fungal Genetics and Biology*
1276 45:68–75.

1277 Wang X, Angelis N, Thein SL. 2018. MYB – A regulatory Factor in Hematopoiesis. *Gene*
1278 665:6–17.

1279 Whitehouse I, Rando OJ, Delrow J, Tsukiyama T. 2007. Chromatin remodelling at promoters
1280 suppresses antisense transcription. *Nature* 450:1031–1035.

1281 Wieser J, Adams TH. 1995. *fibD* encodes a Myb-like DNA-binding protein that coordinates
1282 initiation of *Aspergillus mdulans* conidiophore development. *Genes & Development*
1283 9:491–502.

1284 Willcockson MA, Healton SE, Weiss CN, Bartholdy BA, Botbol Y, Mishra LN, Sidhwani
1285 DS, Wilson TJ, Pinto HB, Maron MI, et al. 2021. H1 histones control the epigenetic
1286 landscape by local chromatin compaction. *Nature* 589:293–298.

1287 Yoshida K, Saunders DGO, Mitsuoka C, Natsume S, Kosugi S, Saitoh H, Inoue Y, Chuma I,
1288 Tosa Y, Cano LM, et al. 2016. Host specialization of the blast fungus Magnaporthe
1289 oryzae is associated with dynamic gain and loss of genes linked to transposable
1290 elements. *BMC Genomics* 17:370.

1291 Zhang L, Zhang D, Chen Y, Ye W, Lin Q, Lu G, Ebbole DJ, Olsson S, Wang Z. 2019.
1292 *Magnaporthe oryzae* CK2 Accumulates in Nuclei, Nucleoli, at Septal Pores and

1293 Forms a Large Ring Structure in Appressoria, and Is Involved in Rice Blast
1294 Pathogenesis. *Frontiers in Cellular and Infection Microbiology* 9:113.

1295 Zhang L, Zhang D, Liu D, Li Y, Li H, Xie Y, Wang Z, Hansen BO, Olsson S. 2019.
1296 Conserved Eukaryotic Kinase CK2 Chaperone Intrinsically Disordered Protein
1297 Interactions. Druzhinina IS, editor. *Appl Environ Microbiol* 86:e02191-19,
1298 /aem/86/2/AEM.02191-19.atom.

1299 Zhao C, Waalwijk C, de Wit PJ, Tang D, van der Lee T. 2014. Relocation of genes generates
1300 non-conserved chromosomal segments in Fusarium graminearum that show distinct
1301 and co-regulated gene expression patterns. *BMC Genomics* 15:191.

1302 Zofall M, Persinger J, Bartholomew B. 2004. Functional Role of Extranucleosomal DNA and
1303 the Entry Site of the Nucleosome in Chromatin Remodeling by ISW2. *Mol Cell Biol*
1304 24:10047–10057.

1305

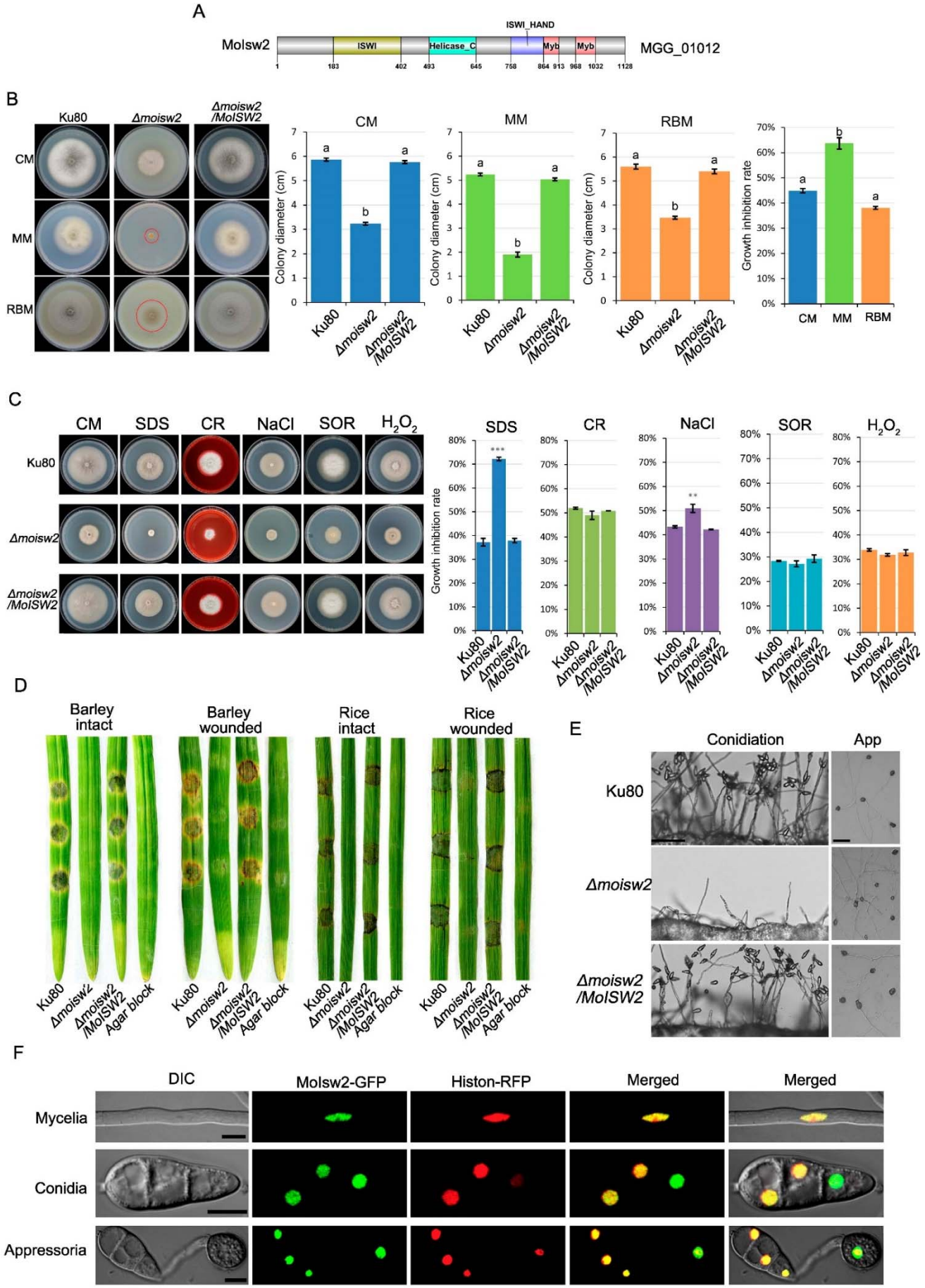
A
MoIsw2
ISWI_HAND
ISWI
Helicase_C
Myb
Myb
MGG_01012
1
183
402
493
645
758
864
913
968
1032
1128
B
Ku80
Δmoisw2
Δmoisw2 /MoISW2
CM
MM
RBM
Colony diameter (cm)
Growth inhibition rate
Ku80
Δmoisw2
Δmoisw2 /MoISW2
C
CM
SDS
CR
NaCl
SOR
H2O2
Ku80
Δmoisw2
Δmoisw2 /MoISW2
Growth inhibition rate
D
Barley intact
Barley wounded
Rice intact
Rice wounded
Ku80
Δmoisw2
Δmoisw2 /MoISW2
Agar block
E
Conidiation
App
Ku80
Δmoisw2
Δmoisw2 /MoISW2
F
DIC
MoIsw2-GFP
Histon-RFP
Merged
Merged
Mycelia
Conidia
Appressoria

1

Figure 1. Domain structure, knockout phenotypes compared to the background Ku80, and localization of MoIsw2. (A) Domain structure (B) Growth phenotypes and growth on complete medium (CM) minimal medium (MM) and rice bran medium (RBM). (C) Stress phenotypes on complete medium (CM) with added Sodium Dodecyl Sulfate (SDS), Congo Red (CR), salt (NaCl), sorbitol (SOR) or hydrogen peroxide (H_2O_2). (D) Infection phenotypes on barley and rice leaves. (E) Conidia formation and appressoria formation from hyphae. (F) Subcellular localization in mycelia, conidia and appressoria MoIsw2-GFP localizes to nuclei (Histon1-RFP nuclear marker). The same letter on the bars indicates $P_{same} > *0.05$. The stars above bars indicate significant differences from the Ku80 controls ** $P_{same} < 0.01$ ***$P_{same} < 0.001$.

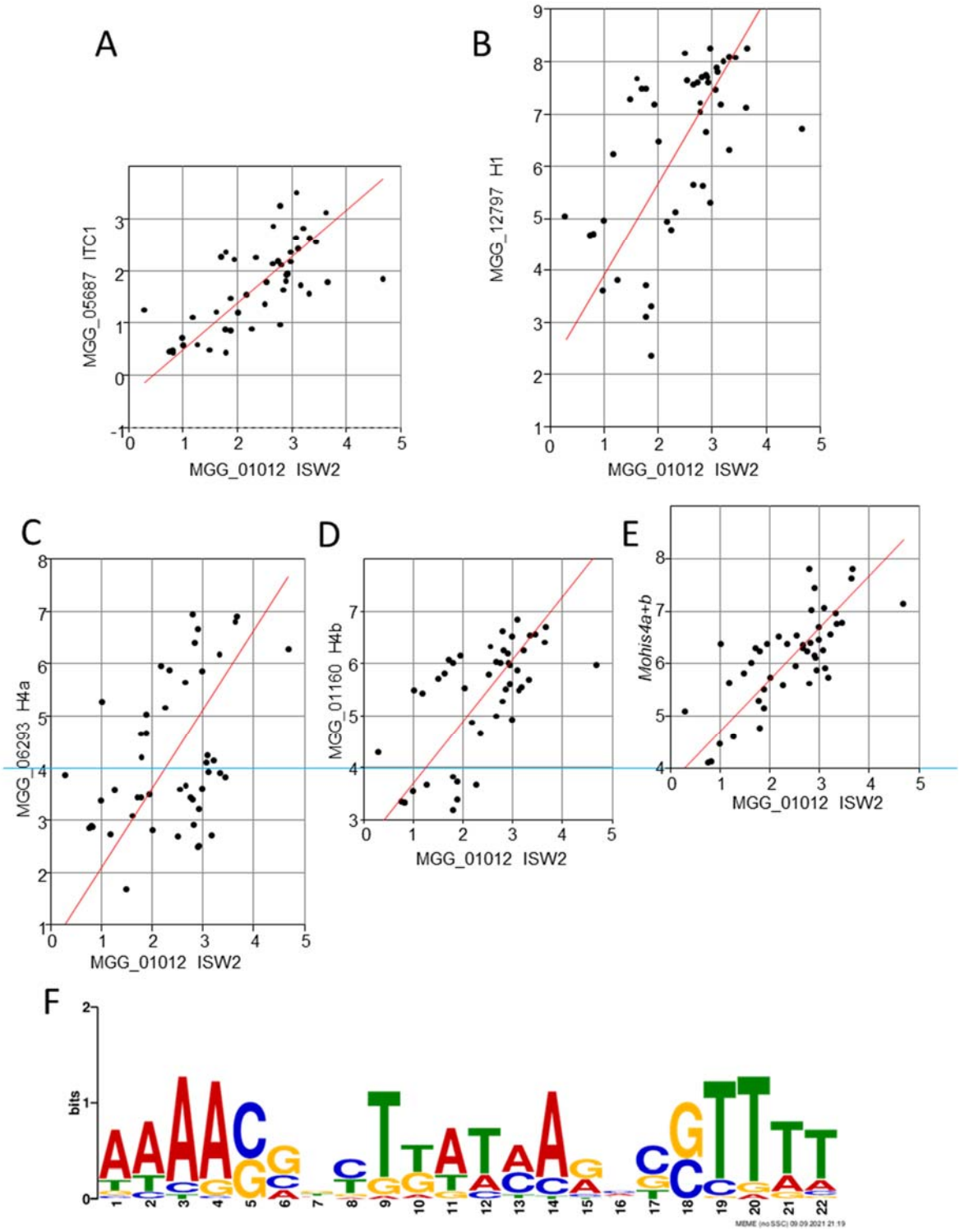

Figure 2. Log2 Reduced Major Axis (RMA) correlations of a putative *ITC1*, the linker histone *HIS1* and the two putative *HIS4* genes putatively expressing the same protein known to interact with the expression of the putative *MoISW2* (x-axis) in published RNAseq data at different stages of plant infection. Each dot represents the two genes'

expression in a separate RNAseq dataset. RMA fitting was used to handle the problem of errors in both X and Y axis values, an inherent consequence of plotting the expression of 2 genes against each other. Each dot corresponds to the value from one transcriptome. (**A**) ITC1, P(uncorrelated)=1.57E-7 (**B**) *HIS1*, P(uncorrelated)=1.48E-5 (**C**) *HIS4a* P(uncorrelated)=0.0044 (**D**) *HIS4b* P(uncorrelated)=3.81E-7 (**E**) *HIS4a* + *4b* since both *HIS4* genes are predicted to encode for the same protein, P(uncorrelated) 5.82E-10. All plots are shown with equal x and y scale gradings so that it is easy to compare slopes between graphs visually. Also, note that figures **C**, **D**, and **E** have been positioned so that Log 4 on the Y-axes are on the same line so that the effect of the addition, Log2(His4a+His4b), can be seen visually. (**F**) A frequently occurring palindromic motif was found in the ChIP-seq data using MoIsw2 as bait. It was found in 196 sequences.

31 **Table 1**. Comparison of the position of avirulence genes compared to the position of
32 the MoIsw2 palindromic DNA binding motif sites in strain Guy11, as well as
33 differential regulation between experiments of the avirulence genes in MoISW2
34 knockout compared to the background, and differential regulation of the same genes
35 during infection of rice in strain Guy11, and strain 98-06 from published data. Blue-
36 marked cells; are genes that MoIsw2 help regulate only in Guy11. Green-marked cells;
37 are genes that are only regulated during infection by 98-06. DelR and VarR contain
38 variation in expression in RNAseq data between mutant and Ku80, and between 55
39 downloaded RNAseq datasets from different labs, respectively (see text below for
40 explanation of these measures). Several of the listed avirulence genes are not present
41 in any of the two strains and some are only present in one of them.
42

ID.	Annotation	Distance from the closest gene to MoIsw2 binding site Guy11	DelR Guy11	Guy11 expr (X)	98-06 expr (X)	VarR Guy11
MGG_12447	cytochalasan	0	19.31	X		48.20
MGG_08386	cytochalasan	NP				
MGG_08377	cytochalasan	NP				
MGG_08378	cytochalasan	1	15.25	X		15.25
MGG_08380	cytochalasan	?			X	
MGG_08381	cytochalasan	?			X	
MGG_08384	cytochalasan	2	0.08	X	X	**29.55**
MGG_08389	cytochalasan	2	2.33	X	X	**24.59**
MGG_08390	cytochalasan	1	0.00	X	X	**56.00**
MGG_08391	cytochalasan	?			X	

MGG_15927	cytochalasan	?			X	
MGG_15928	cytochalasan	NP				

	Avirulence genes					
MGG_07199	ATR13, RxLR effector	170	0.04	X	X	7.27
MGG_10556	Avr_Pii	NP				
MGG_17614	Avr_Pii	NP				
MGG_13283	Avr_Pik	NP				
MGG_15972	Avr_Pik	?			X	
MGG_03029	Avr_Pita1	175	37.08			19.74
MGG_07038	Avr_Pita1	169	2.00			6.25
MGG_09617	Avr_Pita1	NP				
MGG_10927	Avr_Pita1	20	0.07			**24.00**
MGG_03808	Avr_Pita1 like	NP				
MGG_15370	Avr_Pita1 like	1	0.28			**56.00**
MGG_17611	Avr_Pita1	NP				
MGG_14981	AVR_PiTA2	NP				
MGG_15212	AVR_Pita2	?			X	
MGG_18041	Avr_Piz-t	NP				
MGG_03685	Avr-Pi54	238	14.11			3.86
MGG_13863	Avr-PWL1	?			X	
MGG_07398	Avr-PWL2	NP		X		
Sum number	30			7	11	
Only in one of the strains				3	7	
				In both		
				4		

NP=Not Present in Guy11 or 98-06

Bold numbers=Seem to be more important during plant infection

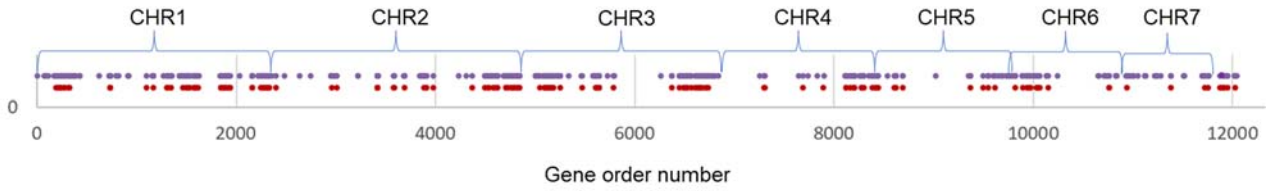

Figure 3. The position of TEs and identified palindromic MoIsw2 binding sites in DNA largely overlap along the whole genome.

58 **Table 1**. Comparison of the position of avirulence genes compared to the position of
59 the MoIsw2 palindromic DNA binding motif sites in strain Guy11, as well as
60 differential regulation between experiments of the avirulence genes in MoISW2
61 knockout compared to the background, and differential regulation of the same genes
62 during infection of rice in strain Guy11, and strain 98-06 from published data. Blue-
63 marked cells; are genes that MoIsw2 help regulate only in Guy11. Green-marked cells;
64 are genes that are only regulated during infection by 98-06. DelR and VarR contain
65 variation in expression in RNAseq data between mutant and Ku80, and between 55
66 downloaded RNAseq datasets from different labs, respectively (see text below for
67 explanation of these measures). Several of the listed avirulence genes are not present
68 in any of the two strains and some are only present in one of them.
69

ID.	Annotation	Distance from the closest gene to MoIsw2 binding site Guy11	DelR Guy11	Guy11 expr (X)	98-06 expr (X)	VarR Guy11
MGG_12447	cytochalasan	0	19.31	X		48.20
MGG_08386	cytochalasan	NP				
MGG_08377	cytochalasan	NP				
MGG_08378	cytochalasan	1	15.25	X		15.25
MGG_08380	cytochalasan	?			X	
MGG_08381	cytochalasan	?			X	
MGG_08384	cytochalasan	2	0.08	X	X	**29.55**
MGG_08389	cytochalasan	2	2.33	X	X	**24.59**
MGG_08390	cytochalasan	1	0.00	X	X	**56.00**
MGG_08391	cytochalasan	?			X	

MGG_15927	cytochalasan	?			X	
MGG_15928	cytochalasan	NP				

	Avirulence genes					
MGG_07199	ATR13, RxLR effector	170	0.04	X	X	7.27
MGG_10556	Avr_Pii	NP				
MGG_17614	Avr_Pii	NP				
MGG_13283	Avr_Pik	NP				
MGG_15972	Avr_Pik	?			X	
MGG_03029	Avr_Pita1	175	37.08			19.74
MGG_07038	Avr_Pita1	169	2.00			6.25
MGG_09617	Avr_Pita1	NP				
MGG_10927	Avr_Pita1	20	0.07			**24.00**
MGG_03808	Avr_Pita1 like	NP				
MGG_15370	Avr_Pita1 like	1	0.28			**56.00**
MGG_17611	Avr_Pita1	NP				
MGG_14981	AVR_PiTA2	NP				
MGG_15212	AVR_Pita2	?			X	
MGG_18041	Avr_Piz-t	NP				
MGG_03685	Avr-Pi54	238	14.11			3.86
MGG_13863	Avr-PWL1	?			X	
MGG_07398	Avr-PWL2	NP		X		
Sum number	30			7	11	
Only in one of the strains				3	7	
				In both		
				4		

NP=Not Present in Guy11 or 98-06

Bold numbers=Seem to be more important during plant infection

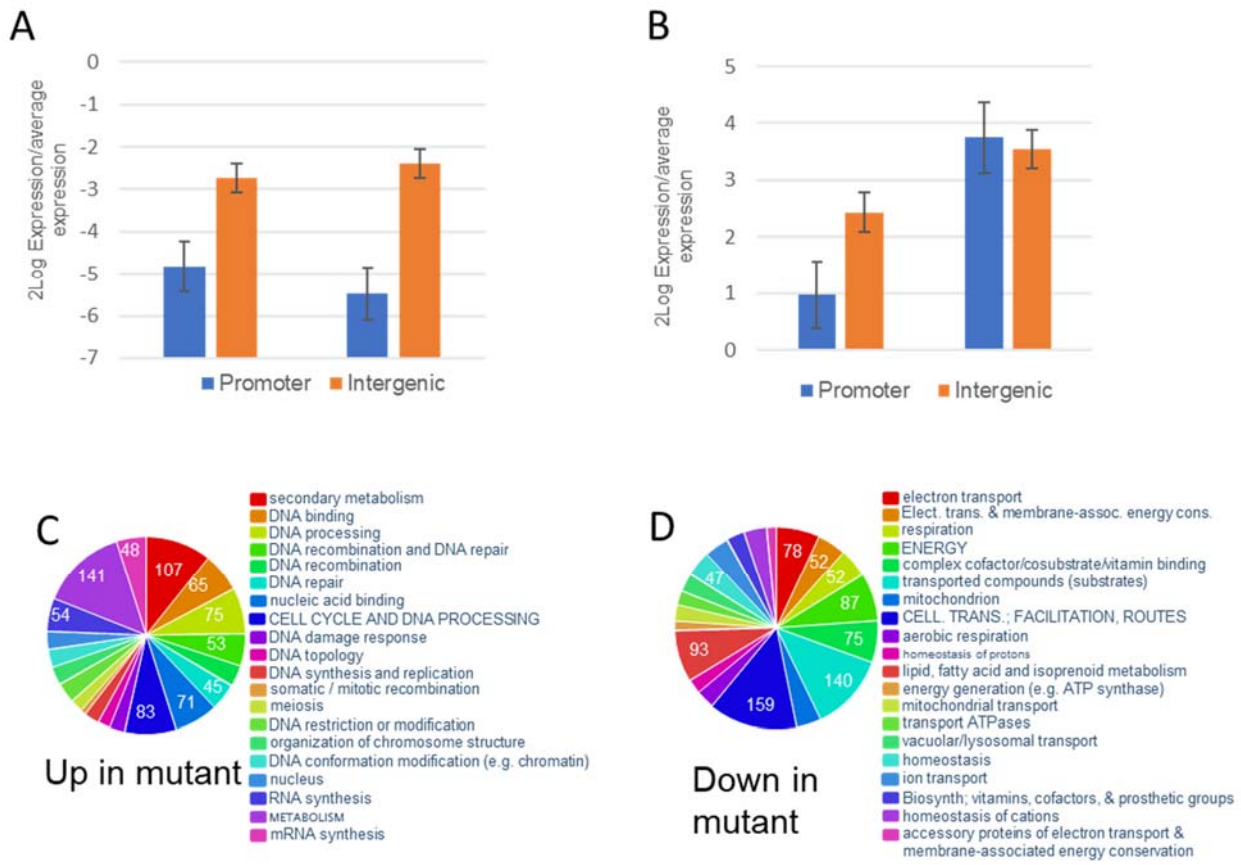

Figure 4. Deletion-induced change in expression of genes next to the predicted palindromic MoIsw2 DNA binding site with hits for the MoIsw2 binding in the ChIP-seq data compared to the average regulation of all genes. (**A**) Expression was, on average higher of genes closest to the binding site in *ΔMoISW2* than Ku80, or with the motif in their promoter region. (**B**) Expression of genes with a binding site in the promoter region and the closest gene when MoIsw2 binding is intergenic. MoIsw2 upregulates both gene types and upregulates genes slightly further away from the binding site, while the absolute (plus or minus) regulation is equal for both types of genes (8-16 times regulation). Error bars indicate SEM (Promoter N=63 Intergenic N=112). (**C**) 20 most significantly enriched upregulated FunCat gene categories in the *ΔMoISW2* compared to the background strain Ku80; Secondary metabolism, DNA-binding, and genes for DNA-related activities and synthesis (anabolism). (**D**)

86 20 Significantly enriched downregulated genes in the mutant are genes for,

87 mitochondrial activities like electron transport and mitochondrial biosynthesis,

88 respiration, and transport routes (catabolism).

89

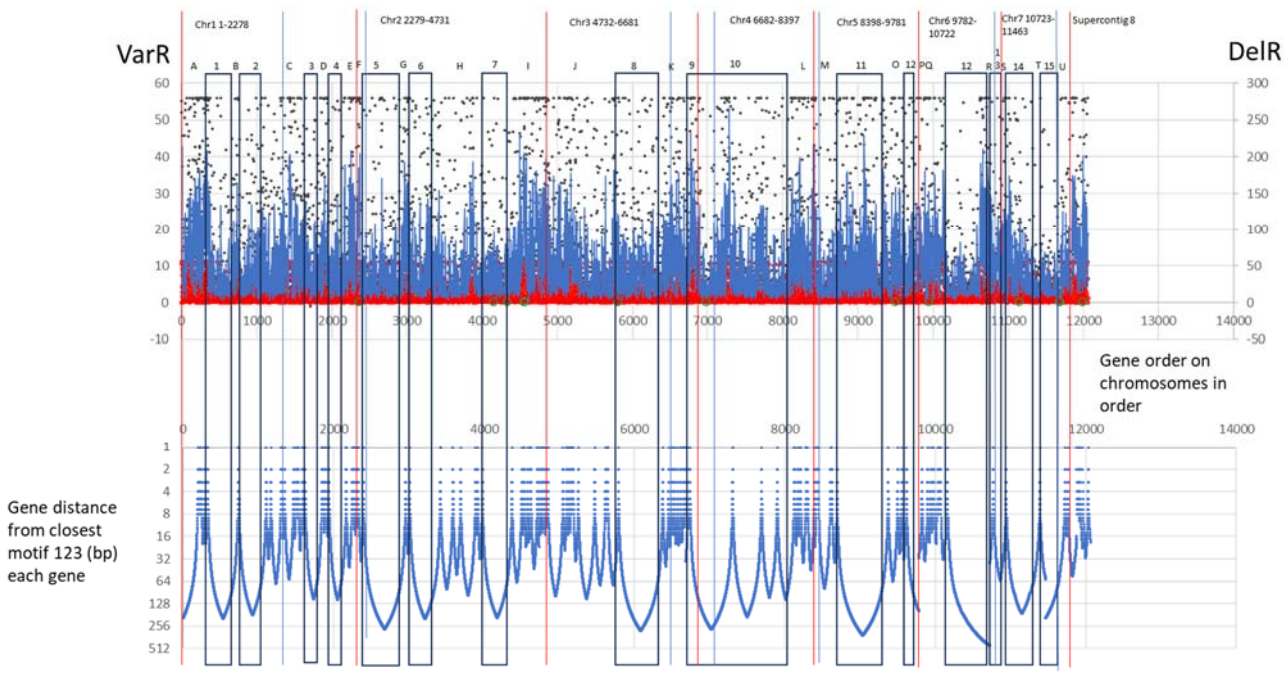

Figure 5. A plot of distances of all genes to the closest motifs of the 123 binding motifs sites (**bottom**) is compared to a plot of the variation of expression across 55 RNAseq experiments (black points and blue 5-point moving average) combined with the difference in gene expression between the *MoISW2* mutant and the Ku80 background (Red points and bright red 5-point moving average (**top**) (DelR). For the VarR data, several genes had at least one condition when their expression was below the detection level while otherwise expressed in these cases the gene expression was set to the lowest detected gene expression. That creates a line of black dots at the top of the figure. The density of the line of dots (top figure) together with areas with less than 16 gene distances from the motif sites paints out the regions of the genome with the most variation in both the VarR and DelR data. The genome contains A-U genomic regions with high variability of gene expression closest (less than 16 genes away) to the MoIsw2 123 DNA binding motifs sites and 1-15 regions with lower variation. Note bottom Y axis is log and reverse, X axis is gene order from 1->12000 on the

105 chromosomes in chromosome order from 1-7 plus supercontig 8 for the whole genome

106 to get the whole genome in order.

107

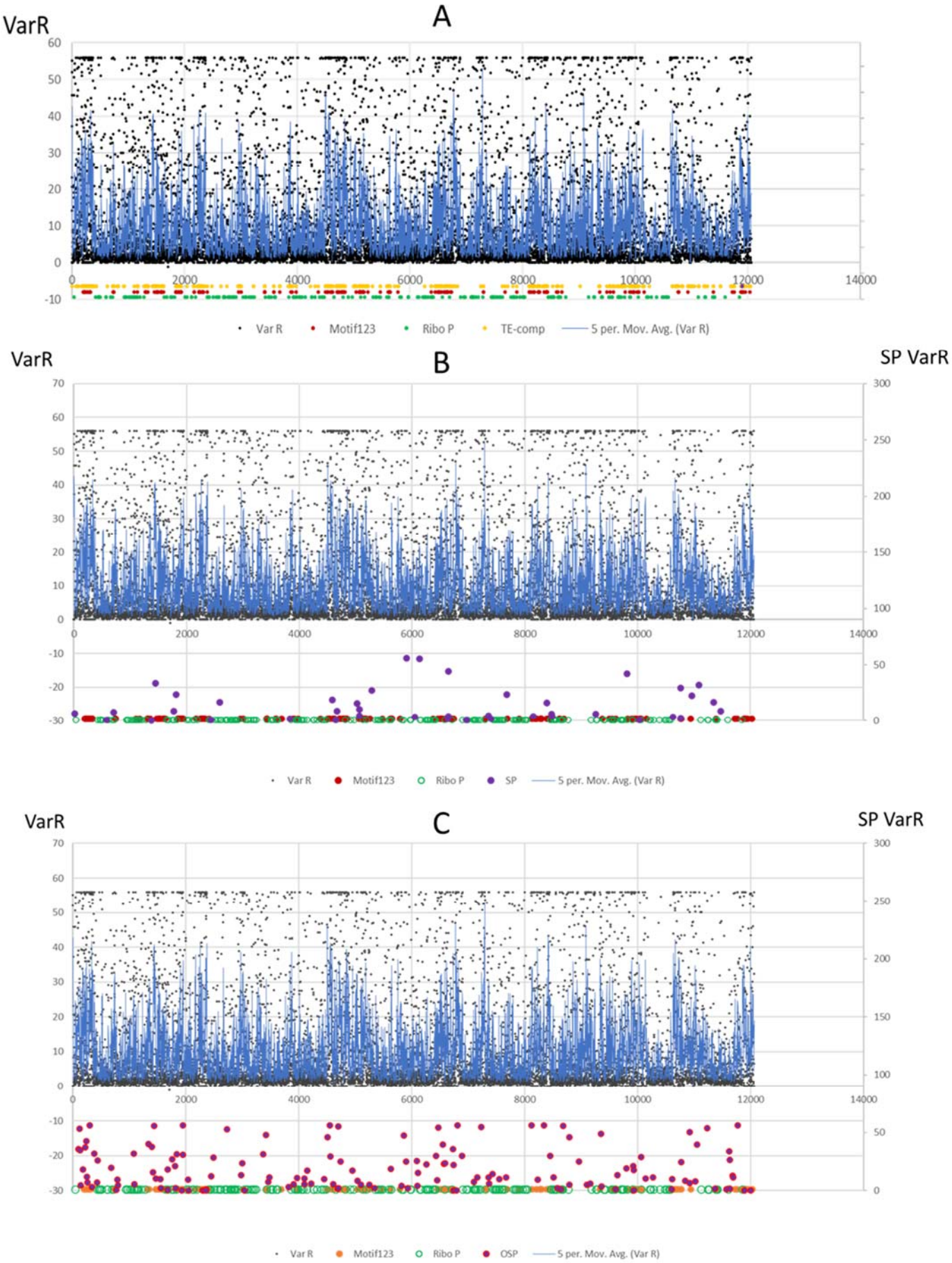
A
VarR
Var R
Motif123
Ribo P
TE-comp
5 per. Mov. Avg. (Var R)
B
VarR
SP VarR
Var R
Motif123
Ribo P
SP
5 per. Mov. Avg. (Var R)
C
VarR
SP VarR
Var R
Motif123
Ribo P
OSP
5 per. Mov. Avg. (Var R)

108

109 **Figure 6**. Position of housekeeping ribosomal genes and genes encoding secreted
110 proteins compared to the position of MoIsw2 DNA binding motifs and genes encoding
111 ribosomal genes compared to VarR variability. (**A**) Ribosomal genes. (**B**) Genes for
112 secreted proteins (SP) with conserved domains (generally larger secreted proteins). (**C**)
113 Genes for other secreted proteins (OSP) without any conserved domains identified
114 (generally small secreted proteins and peptides).
115

116 .

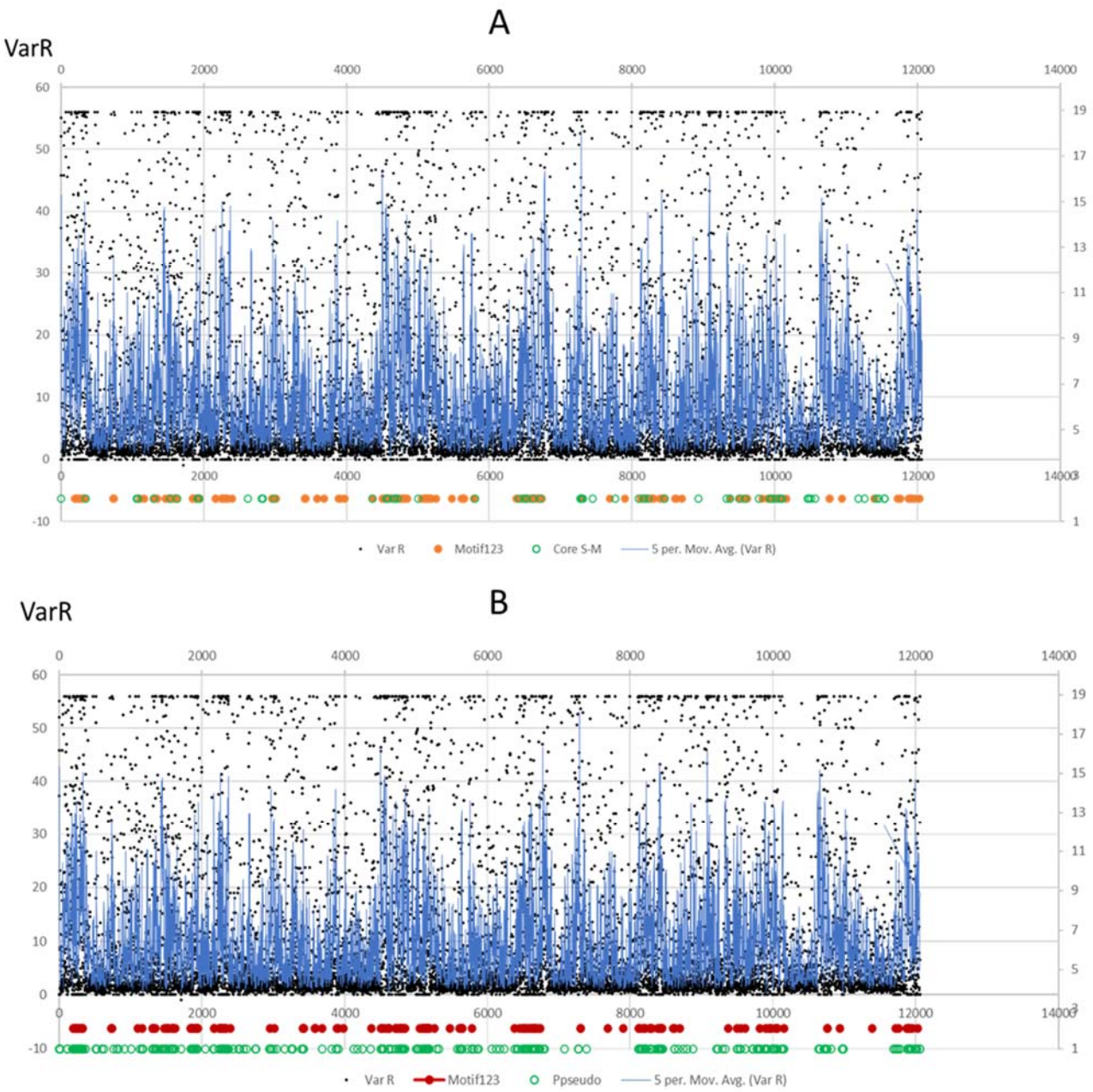

117

118 **Figure 7**. Position of core secondary metabolite genes and potential pseudogenes
119 compared to the position of the MoIsw2 DNA binding motifs and genes encoding
120 ribosomal genes compared to VarR variability. (**A**) Core secondary metabolite genes
121 (green rings). (**B**) Potential pseudogenes not expressed in any treatment (dark green
122 rings). In both A and B, the positions of the 123 MoIsw2 DNA binding motif sites are
123 marked as references.

Table 2. Annotation of the 65 DNA binding genes identified in the analysis shown in Fig. 3C. These 65 genes are the most upregulated in *ΔMoISW2* compared to the expression in the background Ku80-strain. Annotation from NCBI. Note: these are the genes that are most repressed by the MoIsw2 activity.

MGG_ 02762	MGG_02762. ATP-dependent RNA helicase DED1; Belongs to the DEAD box helicase family
MGG_ 06470	MGG_06470, DNA repair helicase RAD25 (835 aa).
MGG_ 05948	MGG_05948 zinc knuckle domain-containing protein. This domain is a zinc-binding domain of the form CxxCxxxGHxxxxC from various species. It is found in the MPE1 protein from Saccharomyces cerevisiae which is a component of the cleavage and polyadenylation factor (CPF) complex important for polyadenylation-dependent pre-mRNA 3'-end formation
MGG_ 01990	b-ZIP transcription factor IDI-4 (induces autophagic cell death in the fungus *Podospora*)
MGG_ 00868	Global Transactivator; Superfamily II DNA or RNA helicase, SNF2 family [Transcription, Replication, recombination and repair];
MGG_ 02429	KOG4062 6-O-methylguanine-DNA methyltransferase MGMT/MGT1, involved in DNA repair Replication, recombination and repair https://jgi-myco-web-4.jgi.doe.gov/annotator/servlet/jgi.annotation.Annotation?pDb=Lasov1&pStateVar=View&pProteinId=680852&pViewType=protein
MGG_ 07015	DNA repair protein Rad7
MGG_ 11518	G/U mismatch-specific uracil DNA glycosylase
MGG_ 04428	Zinc finger transcription factor ace1
MGG_ 07118	sporulation-specific protein 5 (needed for sexual spore formation?)
MGG_ 05995	MGG_05995, Magnaporthe oryzae 70-15 hypothetical protein (244 aa), translin family protein, Translin family (PF01997). If Translin, here is a review about that https://link.springer.com/article/10.1007/s12038-019-9947-6.
MGG_ 04429	ATP-dependent DNA helicase MPH1; ATP-dependent DNA helicase is involved in DNA damage repair by homologous recombination and genome maintenance.

124

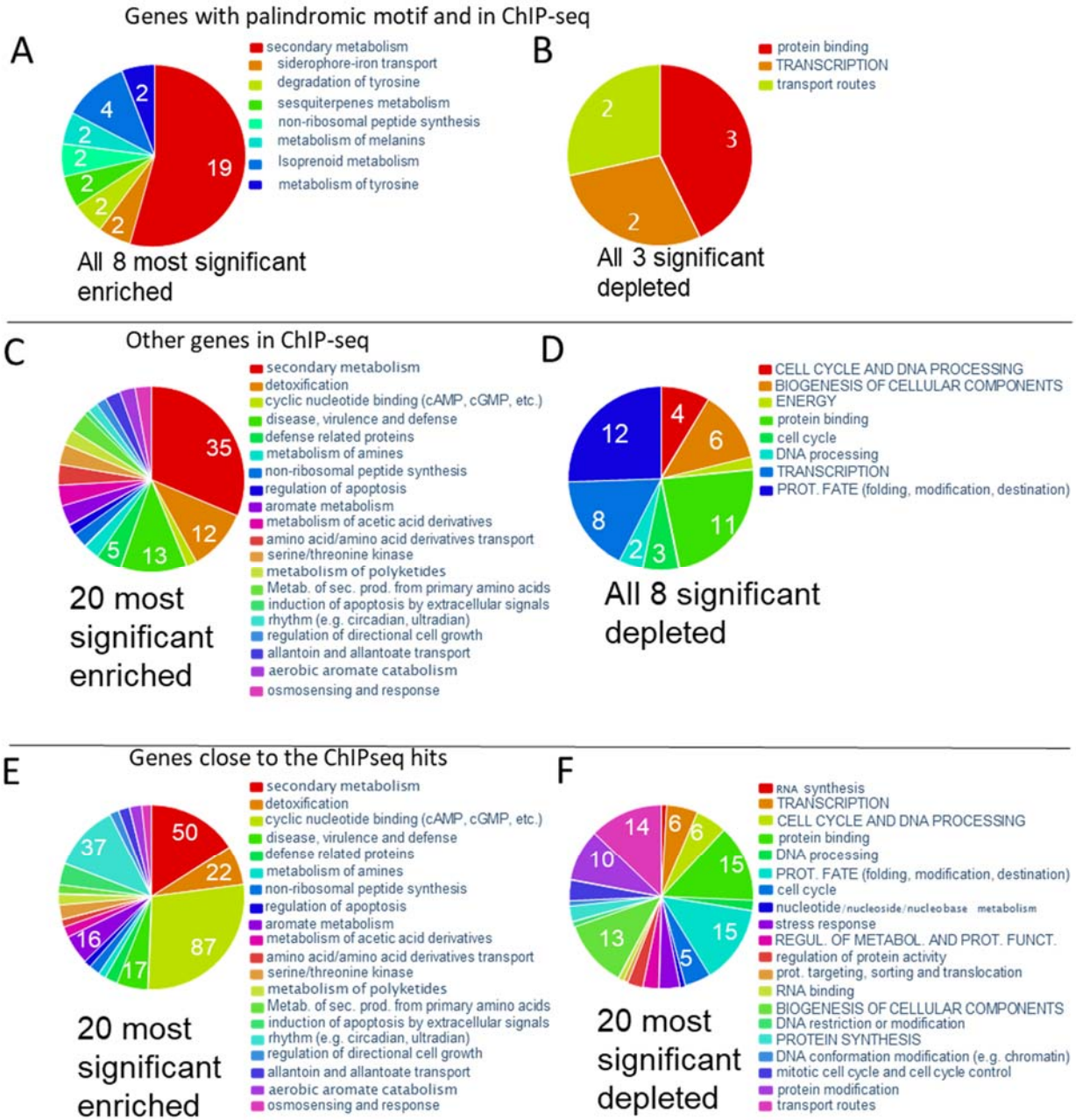

Figure 8. FunCat classification of genes at or close to the MoIsw2 DNA binding sites. (**A**) Significantly enriched and depleted classes of genes in the MoIsw2 ChIP-seq binding assay that also has the MoIsw2 DNA-binding palindromic motif in their upstream region. **(B)** Significantly enriched and depleted classes of all genes with ChIP-seq sequences with MoIsw2 binding to their upstream regulatory DNA

132 sequences. **(C)** Significantly enriched and depleted classes of genes closest to
133 intergenic hits for MoIsw2 binding, excluding the palindromic motif hits
134

.

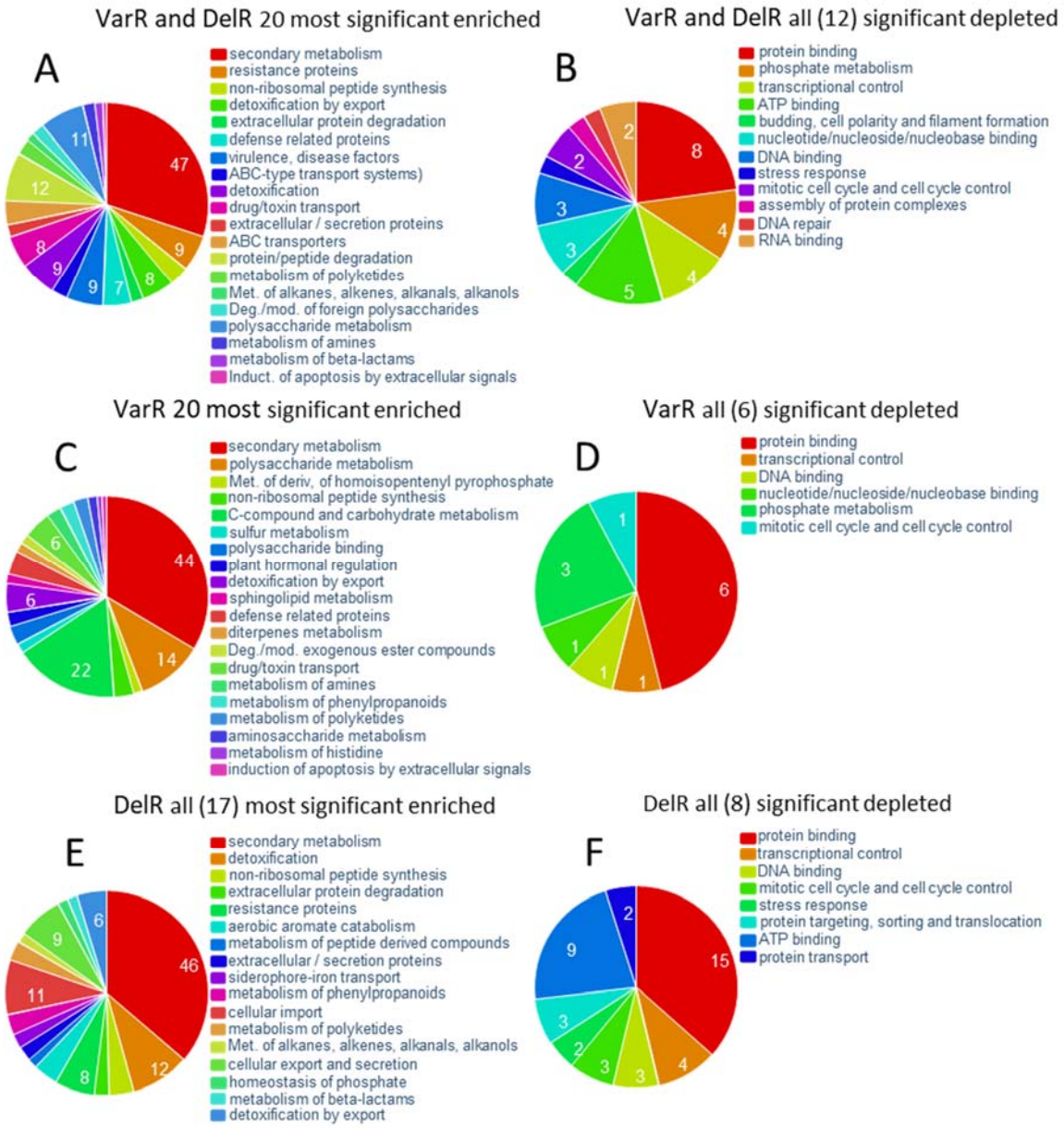

Figure 9. FunCat classification of 500 genes with the most variable gene expression between experiments. (**A**) VarR and DelR enriched. (**B**) VarR and DelR depleted. (**C**) VarR alone Enriched. (**D**) VarR alone depleted. (**E**) DelR alone enriched. (**F**) DelR alone depleted.

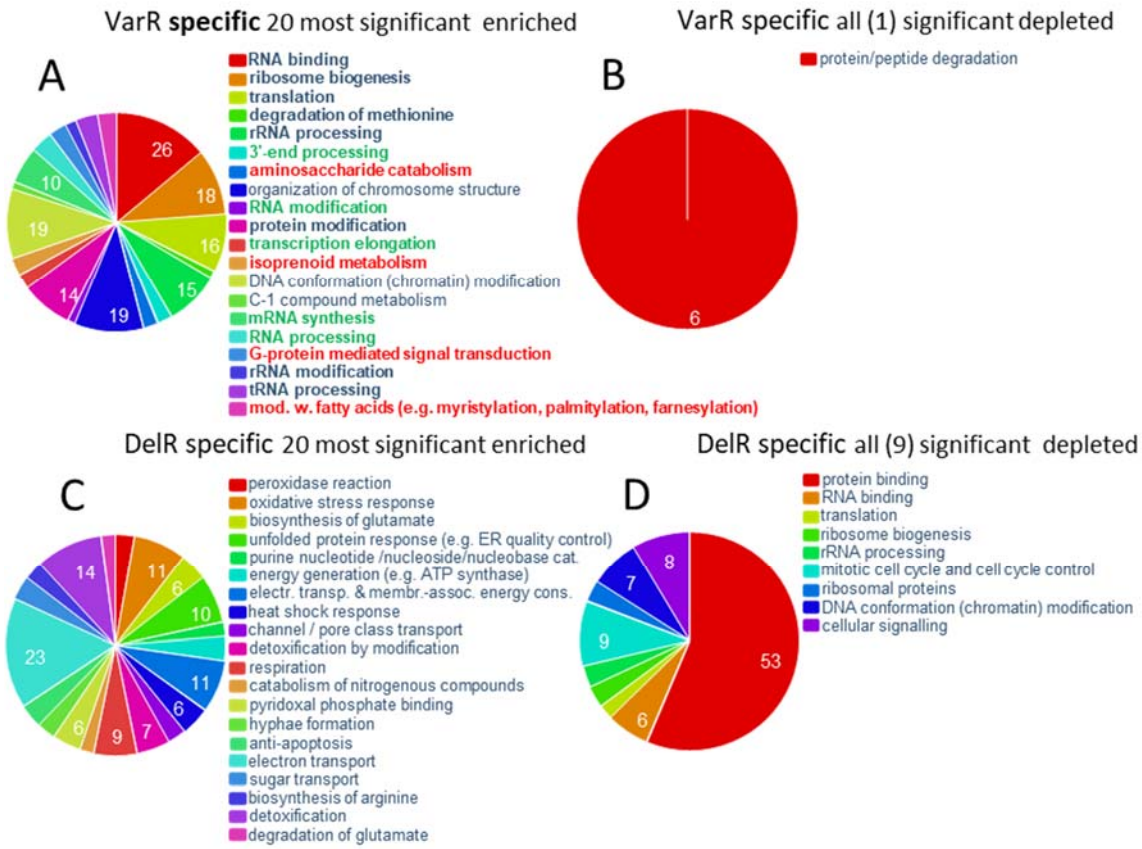

Black bold=translation related

Green bold=transcription related

Red bold=innate immunity related (towards plant? amino saccharide metabolism)

Figure 10 Differences between 500 VarR-specific and DelR-**specific** functional gene classes illustrate the difference in conditions between *in planta* experiments and *in vitro* experiments. (**A**) VarR-specific significantly enriched functional gene classes specifically responding *in planta*. Colour-marked texts are the functional gene classes of special interest for plant pathogenicity (see text). (**B**) VarR-specific significantly depleted functional gene classes specifically responding *in planta*. (**C**) DelR-specific significantly enriched functional gene classes specifically responding *in vitro* (**D**) DelR-specific significantly depleted functional gene classes specifically responding *in vitro*.

Key resources table

REAGENT or RESOURCE	SOURCE	IDENTIFIER
Chemicals, peptides, and recombinant proteins		
MoISW2GFP	This paper	
Critical commercial assays		
ChIP seq service	IGENEBOOK (see this paper supplemental file)	Supplemental Company methods.zip
RNAseq service	IGENEBOOK (see this paper supplemental file)	Supplemental Company methods.zip
Deposited data		
RNAseq compilation of published experiments on gene expressions during infection stages	Zhang et al.[2]	https://doi.org/10.6084/m9.figshare.7068857.v1
ChIPsec data for MoISW2 binding M. oryzae Ku80 DNA RNAseq data for strains ΔMoIsw2 and Ku80 + other supplemental files and analyses 50Mb zip file.	This paper	https://figshare.com/s/df7b6b0bf9caf963a06c reserved DOI https://doi.org/10.6084/m9.figshare.22218328
Magnaporthe oryzae genome, genes sequences and gene contig order data needed to arrange genes in correct order on supercontigs.	BROAD institute	ftp.broadinstitute.org/distribution/annotation/fungi/magnaporthe/genomes/magnaporthe_oryzae_70-15_8 User: Anonymous
Magnaporth oryzae expression Avir genes during rice infection. Strain 98-06	Cao et al. [3]	https://bsppjournals.onlinelibrary.wiley.com/action/downloadSupplement?doi=10.1111%2Fmpp.13224&file=mpp13224-sup-0010-TableS2.xlsx
Sequence downloads, blasts, annotations including domain annotations	NCBI	https://www.ncbi.nlm.nih.gov/
Experimental models: Organisms/strains		
Magnaporthe oryzae (formerly *Magnaporthe grisea*)		Ku80[4] deletion in strain Guy11 NCBI:txid242507
MoISW2-GFP strain derived from Ku80	Li et al. [1]	https://doi.org/10.1101/2021.12.28.474317
Software and algorithms		
PAST statistics software package version 4.08 (released November 2021)	Hammer et al.[5]	https://www.nhm.uio.no/english/research/infrastructure/past/

Microsoft Excel (MS office 365) with Solver Add-In activated	Microsoft	https://www.microsoft.com
Fisher Exact Add-In for MS Excel	software@obertfamily.com	http://www.obertfamily.com/software/fisherexact.html
Other		
FungiFun2 website for Functional Category analysis of putative proteins.	Priebe et al. [6]	https://elbe.hki-jena.de/fungifun/fungifun.php
antiSMASH website for finding core secondary metabolite genes in fungi.	Blin et al. [7]	https://fungismash.secondarymetabolites.org/#!/start
The MEME suite for use of MEME and FIMO	Bailey et al. [8]	https://meme-suite.org/meme/

1. Li, Y. *et al. The* Myb *family genes in the rice pathogen* Magnaporthe oryzae *: Finding and deleting more family members involved in pathogenicity*. http://biorxiv.org/lookup/doi/10.1101/2021.12.28.474317 (2021) doi:10.1101/2021.12.28.474317.
2. Zhang, L. *et al.* Conserved Eukaryotic Kinase CK2 Chaperone Intrinsically Disordered Protein Interactions. *Appl Environ Microbiol* **86**, e02191-19, /aem/86/2/AEM.02191-19.atom (2019).
3. Cao, Y. *et al.* Characterization of two infection-induced transcription factors of *Magnaporthe oryzae* reveals their roles in regulating early infection and effector expression. *Molecular Plant Pathology* **23**, 1200–1213 (2022).
4. Villalba, F. *et al.* Improved gene targeting in Magnaporthe grisea by inactivation of MgKU80 required for non-homologous end joining. *Fungal Genetics and Biology* **45**, 68–75 (2008).
5. Hammer, O., Harper, D. A. T. & Ryan, P. D. PAST: Paleontological Statistics Software Package for Education and Data Analysis. **4**, 9 (2001).
6. Priebe, S., Kreisel, C., Horn, F., Guthke, R. & Linde, J. FungiFun2: a comprehensive online resource for systematic analysis of gene lists from fungal species. *Bioinformatics* **31**, 445–446 (2015).
7. Blin, K. *et al.* antiSMASH 6.0: improving cluster detection and comparison capabilities. *Nucleic Acids Research* **49**, W29–W35 (2021).
8. Bailey, T. L., Johnson, J., Grant, C. E. & Noble, W. S. The MEME Suite. *Nucleic Acids Res* **43**, W39–W49 (2015).